Structures 86 (2026) 111279

Contents lists available at ScienceDirect

Structures

journal homepage: www.elsevier.com/locate/structures

A proposal for the calibration of the Italian seismic action in accordance with a reliability-based design procedure

Matteo Tatangelo [a,1,*], Lorenzo Audisio [a,2], Michele D'Amato [b,3], Rosario Gigliotti [a,4], Franco Braga [a]

[a] DISG, Dept. of Structural and Geotechnics Engineering, Sapienza University of Rome, Via Eudossiana 18, Rome 00184, Italy
[b] DIUSS, Dept. for Humanistic, Scientific and Social Innovation, University of Basilicata, Via Lanera, Matera 75100, Italy

ARTICLE INFO

Keywords:
Seismic reliability
Seismic risk
Seismic design
Target reliability index
Partial factors

ABSTRACT

In Italy the current seismic design standards for new and existing constructions relies on *Uniform-Hazard Approach* (*UHA*), assigning fixed hazard-exceedance probabilities to different *Limit States* (*LSs*). However, this approach leads to non-uniform seismic risk, since failure probabilities vary across a territory depending on local seismic hazard conditions. To cover this gap, this study proposes a reliability-based procedure for calibrating the seismic action of constructions, consistent with the probabilistic framework of SAC FEMA and the *Risk-Targeted Approach* (*RTA*). In accordance with this procedure, target reliability indexes and the corresponding reliability factors are proposed by referring to the current *MPS-04* seismic hazard model. To this scope exceedance probabilities for different *LSs* and *Consequence Classes* (*CCs*) are defined, and the seismic hazard function parameters are optimized in a log–log space. Assuming the annual failure probability of 2×10^{-4} provided by FEMA, average target reliability factors of 2.11 for the *Ultimate Limit State* (*ULS*) and 1.0 for the *Serviceability Limit State* (*SLS*) are obtained for the Italian territory. Based on these values, mean target reliability indexes are then derived as functions of the *LS* and *CC*. The results obtained clearly show that, coherently with the *UHA*, the *Expected Annual Losses* (*EALs*) and reliability indexes vary significantly across Italy, indicating a non-uniform risk distribution. Conversely, the reliability-based procedure achieves uniform seismic risk by introducing a site-specific modification factor to the MPS-04 seismic action. The reliability factors derived according to the proposed design procedure may be readily implemented in the design code to calibrate a seismic action ensuring a uniform seismic risk across the Italian territory.

1. Introduction

To date, the main international codes employ the *Uniform-Hazard Approach* (*UHA*) in constructions design, where the seismic action is defined by means of response spectra having an equal exceedance probability in a certain reference period [1–3]. This implies that, although structures result code-conforming with the required seismic strength, they offer a different failure probability [4–7].

On the contrary, new generations of standards are increasingly emphasizing approaches for uniform risk design and assessment across a territory. Recently, several works proposed to abandon the *UHA* and to calibrate the seismic action to achieve a specific requirement in terms of failure probability related to a specific structural performance. This approach, called *Risk-Targeted Approach* (*RTA*) [8,9], implies the choice of an appropriate failure probability (annual or over a certain reference period) as a probabilistic requirement target for a given a *Limit State* (*LS*). This requirement is met by employing a specific fragility curve representing the conditional failure probability for a given *Intensity Measure* (*IM*).

SAC Federal Emergency Management Agency [10] proposed a formal probabilistic framework for seismic design and assessment of steel moment-resisting frame buildings, based on the reliability-targeted

* Corresponding author.
E-mail address: matteo.tatangelo@uniroma1.it (M. Tatangelo).
[1] 0000-0001-5162-4073
[2] 0000-0002-3232-0688
[3] 0000-0003-31076262
[4] 0000-0002-2967192X

https://doi.org/10.1016/j.istruc.2026.111279
Received 10 October 2025; Received in revised form 13 December 2025; Accepted 1 February 2026

approach described by Cornell et al. [11]. According to this framework, as alternative to the convolution integral a closed-form solution was proposed for calculating the structural failure probability, by adopting some simplified assumptions on the seismic hazard law and probability distribution of demand and capacity. Precisely, as for the seismic hazard law the formulation proposed by Sewell, Toro, & McGuire [12] was introduced, considering a power law for linearly fitting the site seismic hazard in a log-log plane. In this regard, some criticism was made by Aslani & Miranda [13] and Bradley & Dhakal [14]. In particular, validity of approximation used to derive the seismic hazard curve in closed form was questioned, due to its lack of accuracy when the seismic hazard data have large curvatures. To date, other more detailed formulations for the seismic hazard law are proposed. For instance, in the log-log plane in Bradley et al. [15] a hyperbolic law was proposed, while in Vamvatsikos [16] a second-order polynomial law was adopted. Further developments of the formal probabilistic framework originally introduced by Cornell et al. [11] were provided in Torres & Ruiz [17], Celarec, Vamvatsikos, & Dolšek [18] and Vamvatsikos & Dolšek [19], where the time-dependent variations in structural capacity were included. Also, in Tolentino, Ruiz, & Torres [20] and Tolentino & Ruiz [21] uncertainties in both seismic demand and capacity were simultaneously considered. Celarec & Dolšek [22] derived a closed-form expression to estimate the mean annual failure rate of reinforced concrete frames with masonry infills, while Fragiadakis et al. [23] proposed an alternative analytical formulation based on a linear approximation of the hazard curve. More recently, Flores & Tolentino [24] introduced mathematical expressions that normalize capacity and demand into a single dependent variable, enabling the estimation of the expected mean failure rate without resorting to convolution.

As far as the fragility curves are concerned, they represent an important tool within a probabilistic approach [25,26]. They may be determined with *Incremental Dynamic Analysis* (*IDA*), where a relationship between *IM* and *Engineering Demand Parameters* (*EDP*) procedure may be utilized [27]. To this scope, a set of accelerograms is chosen, amplified or scaled to estimate the structural response for different *IMs*. Similar results can be obtained with the *Multiple Stripe Analysis* (*MSA*) method, where accelerograms records are scaled in relation to a common *IM* [28], or with the *Cloud* method, where unscaled accelerations and linear regressions are used [11,29]. However, given complexity and high computational efforts required, simplified tools for fragility curves construction are proposed, too. Among these, in Baltzopoulos et al. [30] the *SPO2FRAG* approach is presented. Whereas, in Vamvatsikos & Cornell [31] the *SPO2IDA* approach is proposed, for deriving approximated *IDA* results obtained from *Static Push-Over* (*SPO*). Another possible approach consists in the use of an *Incremental N2* (*IN2*) curve [32,33], which is intended to approximate a mean *IDA* curve, where fragility curves may be determined with the default values assumption for dispersion measures [34].

Research on construction vulnerability and risk is a topic of growing relevance worldwide. For example, notable studies were conducted based on damage observed after seismic events in Albania [35], Croatia [36], China [37], Chile [38,39], and Italy [40–42]. Furthermore, also investigations on seismic reliability of isolated constructions were conducted in Castaldo & Ferrentino [43] and Micozzi et al. [44]. Recently, effectiveness of data-driven methods for estimating seismic response is considered. To this regard, the information-theory-guided machine--learning approach proposed by De Iuliis, Miceli & Castaldo [45] showed and improved predictive capability for nonlinear single degree of freedom systems, indicating that such techniques may complement and strengthen reliability-based seismic assessments.

Recently, in Žižmond & Dolšek [7] numerical formulations are proposed for the reliability-targeted design spectral acceleration definition to be applied within the force-based method. More in detail, in the direct formulation the spectral acceleration is obtained by means of a convolution integral of a fragility curve and seismic hazard. Whereas the indirect formulation is based on closed-form solution of Cornell et al. [11]. The latter is proposed when the seismic hazard is defined by the traditional uniform seismic hazard maps related to a specific return period T_R (e.g. [1–3]). Then, starting from a target reliability index (or target failure probability), the reliability-targeted design spectral acceleration is obtained by means of a reliability factor [7,46].

Although these formulations are clear to date does not exist an explicit proposal of target reliability indexes for *LSs* and *Consequence Classes* (*CCs*) within an *RTA* [8,9]. This absence makes it difficult to define directly the seismic action that guarantees a uniform failure probability across a territory having a site-by-site different seismic hazard. Among the few documents available, ASCE [47] provides the value of 2×10^{-4} for annual *Near Collapse* (*NC*) exceedance probability, having a 2 % hazard-exceedance probability in 50 years (i.e., a 0.04 % annual probability) for U.S.A. The same value is also found in the Model Code [48] and in the second-generation of Eurocode 8 [49]. In Europe, studies for the definition of reliability-targeted seismic design maps are carried out in France [50], Spain [51] and for the entire European territory [52]. Similar work may be found also in China [53], New Zealand [54,55], Iran [56,57] and U.S.A. Luco et al., [58]. Moreover, Franchin & Noto [59] introduce a partial factors formulation to achieve a target reliability when using the displacement-based approach.

In the current Italian seismic design standards [3], seismic actions are determined using a *UHA* applied across the entire national territory. Under this methodology, response spectra are calibrated with a fixed exceedance probability over the certain reference period. Therefore, the standards are based on seismic hazard maps developed for multiple return periods T_R, where the intensity measure is typically expressed in terms of peak ground acceleration a_g on rigid soil and several spectral acceleration values. Despite ensuring code compliance in terms of required seismic resistance, this approach does not guarantee a uniform level of structural reliability, since the resulting failure probability significantly varies site-by-site [5,6].

This paper presents a reliability-based procedure for calibrating the design seismic action for constructions, allowing us to meet specific reliability requirements. It is based on the approach described in FEMA [10] and found in Cornell et al. [11], providing a formal probabilistic framework for defining the annual exceedance rate of seismic action as a function of *LS* and *CC*. In this work this probabilistic framework is applied to the Italian context (*MPS-04* seismic hazard model, [60]) and extended to reference periods larger than one year. This allows to derive the target reliability indexes and corresponding target reliability factors required to define a design seismic action across the Italian territory satisfying a uniform failure probability. In this way, it is possible to pursue a reliability-based seismic design approach across Italy, a method currently absent from Italian standards and typically addressed by *RTA* [8,9]. Moreover, the procedure would cover the gap so that designing for both vertical loads and seismic conditions would fall within a common reliability framework based on the partial factors approach, considering the same reference period. An overstrength factor to calibrate the target reliability factors is also considered, that would make possible to take into account the overstrength reserve in constructions, achievable through the partial factors. Finally, also a seismic risk analysis across the Italian territory is conducted, by comparing the results obtained with the *UHA* with the *RTA* ones, where the target reliability factors calibrated with the procedure proposed are applied.

To ensure a specific target reliability index the reliability-targeted modification factor is site-dependent, because the seismic hazard and, consequently, the seismic spectra are also site-dependent. Several studies have shown that unlike uniform hazard spectra the modified ones can significantly guarantee a specific reliability and reduce the spatial variability of seismic risk (e.g. [7,50,51,58]). The aim of this work is to quantify the reliability-targeted modification factor for the Italian context.

To address these aspects, the work presented in this paper develops a reliability-based procedure for the calibration of seismic design actions in Italy. The study is articulated in the following main stages. Firstly, the

probabilistic framework proposed in FEMA [10] and Cornell et al. [11] is recalled and extended to reference periods larger than one year, enabling the definition of target reliability factors for different *LSs* and *CCs*. Then, the framework is applied to the Italian *MPS-04* seismic hazard model to derive the corresponding seismic hazard function parameters and to quantify the target reliability factors over the national territory. In this way, the target reliability indexes are calibrated based on different performance levels, accounting for uncertainties in structural capacity and demand. Finally, the proposed reliability-targeted seismic actions are compared to those currently adopted in Italian standards, by means of a seismic risk assessment across the national territory, highlighting the framework effectiveness in achieving uniform seismic risk over the national territory. In this way, the work presented covers the existing gap between seismic and vertical loads design, allowing both actions to be consistently defined within a common reliability framework based on the partial factor approach and referring to the same design reference period.

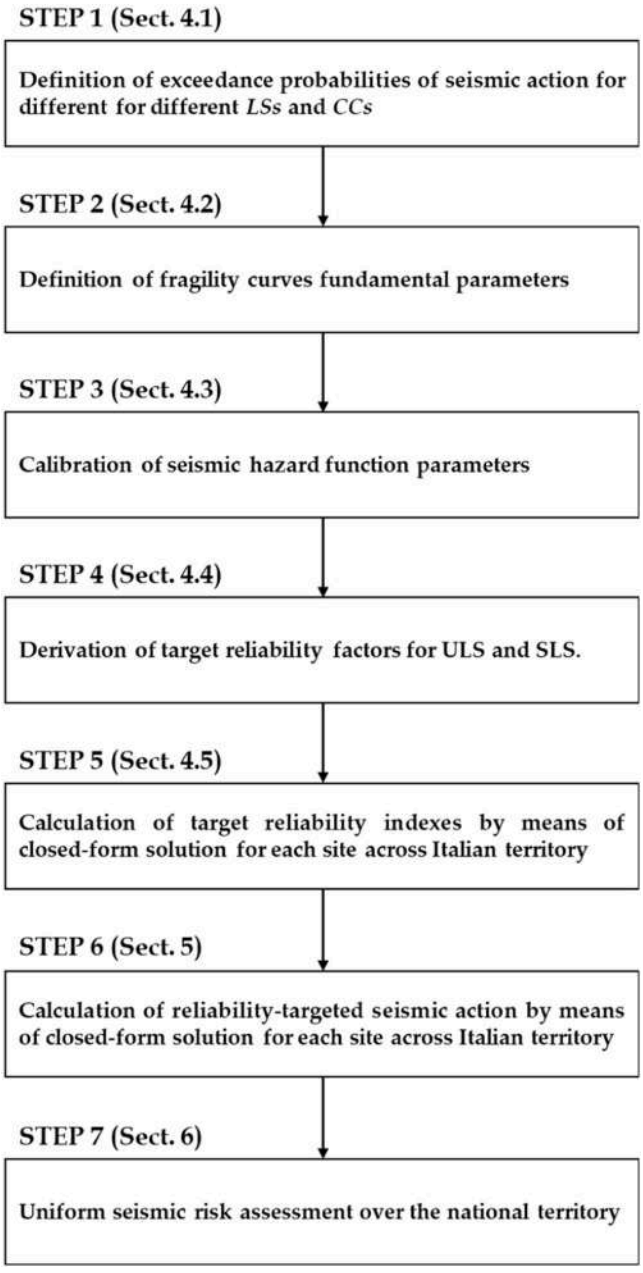

Fig. 1. Comprehensive workflow of the proposed reliability-based procedure for seismic action calibration.

Fig. 1 illustrates the complete workflow of the proposed reliability-based procedure, providing a comprehensive overview of the methodology from the initial definition of design parameters to the final seismic risk assessment and validation of results.

2. Methodology

Let assume that the structural problem on a construction subjected to an earthquake motion is formalized within a probabilistic approach, where epistemic (model and test data variability, knowledge, etc.) and aleatory (record-to-record variability) uncertainties are taken into account. The failure probability may be calculated through the convolution integral of seismic hazard and vulnerability, by using the total probability theorem [61]. If the displacement demand D and capacity C measuring the maximum inter-story drift are separately considered [11], then the annual failure probability P_{f1} of a certain *Limit State* (*LS*) may be derived according to the Eq. 1 [11,25]:

$$P_{f1} = \int P[C \le edp] \cdot |d\lambda_D(edp)| = \int \Phi\left[\frac{\ln\left(\frac{edp}{\widehat{C}}\right)}{\sigma_{\ln}}\right] \cdot |d\lambda_D(edp)| \quad (1)$$

where $|d\lambda_D(edp)|$ is the differential absolute value of the drift demand hazard curve $\lambda_D(edp_i)$, obtained with the Eq. 2 [11]:

$$\lambda_D(edp) = \int P[D \ge edp | IM = im] \cdot |d\lambda_H(im)| \quad (2)$$

$|d\lambda_H(im)|$ indicates the absolute value of the differential of the site ground motion hazard curve $\lambda_H(im)$. The absolute value is considered because the site ground motion curve has a negative derivative. In the Eq. 1 $\Phi[\bullet]$ is the standard normal cumulative distribution representing the fragility curve lognormally distributed, having a median value $\widehat{C}$ (50 % cumulated probability) and $\sigma_{\ln}$ as logarithmic values standard deviation (representing the fragility function shape). The integrals of Eq. 1 and Eq. 2 are expanded, respectively, over all possible values of the engineering demand parameter edp_i (e.g. inter-story drift) and of the ground motion intensity measure im_i.

The P_{f1} may be calculated through the Eq. 1 once $\sigma_{\ln}$, $\widehat{C}$ and $\lambda_H(im)$ are known. Alternatively, Cornell et al. [11] proposed, in a closed form, an approximated formulation for solving P_{f1}, involving a simplified expression for the site seismic hazard function $\lambda_H(im)$ and for the *edp* median value indicated as $\widehat{D}$.

As far as the seismic hazard function $\lambda_H(im)$ is concerned, the power law expression proposed by Sewell, Toro, & McGuire [12] was adopted (Eq. 3). Currently, this formulation is also widely reported in several standards, linking the exceedance annual rate to the ground-motion intensity in the following way:

$$\lambda_H(im) = k_0 \cdot (im)^{-k_1} \quad (3)$$

where k_0 and k_1 are empirical positive constants representing, respectively, the intercept and the slope of the function that is linear in a log-log plane. However, it should be mentioned that in literature to date more complex formulations of the seismic hazard curve are also proposed such as, among the others, the formulations proposed in Bradley et al. [15] and Vamvatsikos [16]. Note that the Eq. 3 includes the site effects on the *im* considered. Therefore, k_0 and k_1 are constants taking into account the site effects, different from the ones evaluated with respect to the rigid subsoil.

In addition, in Cornell et al. [11] the following relationship for structural performance was assumed (Eq. 4):

$$\widehat{D} = a \cdot (IM)^b \quad (4)$$

where $\widehat{D}$ is the *edp* median value conditional to the *IM*. a and b are positive constants obtained from numerical regression of the non-linear structural analyses (*IDA*, Cloud analysis, etc…), and b describes the structural response non-linearity. The parameter b implicitly captures non-linear structural behaviors including yielding and plastification of members, stiffness degradation from cracking, strength deterioration under cyclic loading, and P-Δ effects. When $b = 1$ the structure follows a linear trend between *edp* and *im*. This assumption becomes particularly suitable when the equal displacement rule is satisfied. b is generally larger than 1 for structures with short fundamental period where showing a more pronounced non-linear displacement [62].

By replacing the Eq. 3 and the Eq. 4 (the latter by substituting $\widehat{C}$ for $\widehat{D}$) into the Eq. 1, the following closed form of P_{f1} (Eq. 5) is obtained [11]:

$$P_{f1} = k_0 \cdot (im_{\hat{C}})^{-k_1} \cdot \exp\left(\frac{{k_1}^2 \cdot {\sigma_{\ln}}^2}{2 \cdot b^2}\right) \tag{5}$$

where $im_{\hat{C}}$ may be assumed equal to the median intensity measure corresponding to $\widehat{C}$ [7]. Therefore, P_{f1} may be calculated with the Eq. 5 once the coefficients (k_0, k_1), the fragility function shape ($\sigma_{\ln}$) and the *LS* threshold $im_{\hat{C}}$ are known.

As known, within a reliability-based procedure it is required to define for each *LS* a seismic action as function of a desired target reliability within a certain *reference period* (t_{ref}) longer than one year. This would permit to achieve a reliability-targeted seismic design useful for the life-cycle management of new and existing constructions. To this regard, it should be mentioned that recently a new methodology for life-cycle assessment of constructions considering only vertical loads was proposed in [63]. For this reason in this paper the development of a methodology for deriving reliability-targeted seismic actions is presented, providing the missing methodology to obtain a complete framework for life-cycle management of constructions including vertical loads and seismic action. To this scope, the methodology here presented, differently from the Eq. 5, refers to a target reliability within a certain t_{ref} and not for one year.

In order to define for a construction a specific failure probability target, the *safety factor* γ_{edp} [7,46] is introduced (Eq. 6), expressed as follows:

$$\gamma_{edp} = \frac{\widehat{C}}{\widehat{D}} = \left(\frac{im_{\hat{C}}}{im_{\hat{D}}}\right)^b \tag{6}$$

If $im_{\hat{C}}$ is unknown, then the Eq. 6 may be rewritten in the following way (Eq. 7):

$$im_{\hat{C}} = \gamma_{edp} \cdot (im_{\hat{D}})^{1/b} \tag{7}$$

where $im_{\hat{C}}$ is a function of $im_{\hat{D}}$, the latter evaluated by means of the traditional uniform seismic hazard maps (i.e. by using the *UHA*) referred to specific value of $\lambda_H(im_{\hat{D}})$ (e.g. [1–3]).

By deriving $im_{\hat{D}}$ from the Eq. 3 and by substituting into the Eq. 7, the Eq. 5 becomes (Eq. 8):

$$P_{f1} = \frac{\lambda_H}{{\gamma_{edp}}^{k_1/b}} \cdot \exp\left(\frac{{k_1}^2 \cdot {\sigma_{\ln}}^2}{2 \cdot b^2}\right) = \Phi(-\beta_1) \tag{8}$$

where β_1 is the annual *reliability index* [64]. Moreover, the previous equation may be rewritten also in terms of seismic action return period T_R, by substituting the term $1/T_R$ to the exceedance annual rate λ_H.

Therefore, once P_{f1} is calculated β_1 is obtained with Eq. 9:

$$\beta_1 = -\Phi^{-1}(P_{f1}) \tag{9}$$

It is useful to study how β_1 (Eq. 9) may vary with the parameters k_1, $\sigma_{\ln}$, b, and γ_{edp} (Eq. 8). To this aim, Fig. 2 reports the β_1 values considering $\lambda_H =$ 0.0021 1/years (that is 1/475 years) and by fixing γ_{edp}

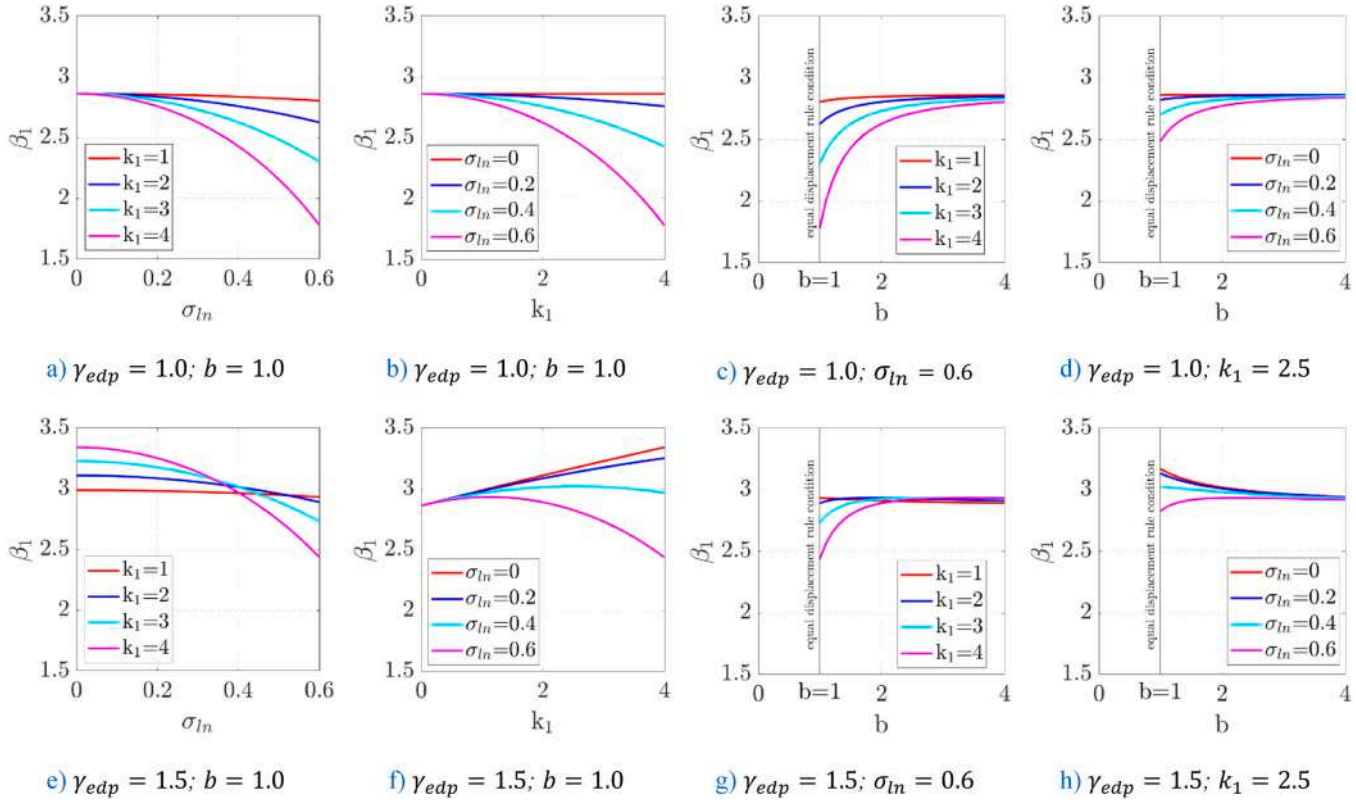

Fig. 2. Annual reliability index (β_1) as function of seismic hazard slope (k_1), fragility dispersion ($\sigma_{\ln}$), structural non-linearity (b), and safety factor (γ_{edp}) for λ_H = 0.0021 year^{-1} (T_R = 475 years): a-d) γ_{edp} = 1.0; e-h) γ_{edp} = 1.5.

equal to either 1 (Fig. 2.a-d) or 1.5 (Fig. 2.e-h). In these graphs several values of k_1 (such as 1, 2, 3, 4) and $\sigma_{\ln}$ (0, 0.2, 0.4, 0.6) are considered.

As it can be observed β_1 is strongly influenced by the value of γ_{edp} rather than the values of $\sigma_{\ln}$ and k_1. Indeed, by comparing Fig. 2a and e, b and f, c and g, d and h, the β_1 trend changes significantly as γ_{edp} changes from 1.0 to 1.5. More in detail, when $\gamma_{edp} = 1$, β_1 decreases (or alternatively P_{f1} increases) by increasing $\sigma_{\ln}$ (Fig. 2a), while β_1 increases as k_1 (Fig. 2b) and b (Fig. 2c and d) increase. In the case of Fig. 2e, if $\gamma_{edp} = 1.5$, β_1 decreases by increasing $\sigma_{\ln}$, similarly to the Fig. 2a. Whereas, in the case of the Fig. 2f, g and h a clear trend of β_1 is not observed by increasing k_1 and b, respectively.

If the annual reliability β_1 is known then the reliability requirement for a given *LS* is known. In this case $\beta_1 = \overline{\beta}_1$, where the notation $\overline{\beta}_1$ is introduced for specifying that the annual target reliability index is known. Hence, the Eq. 8 may be turned by deriving $\gamma_{edp}(\overline{\beta}_1)$ (Eq. 10), that may defined as the *target reliability factor corresponding to* $\overline{\beta}_1$ [7]:

$$\gamma_{edp}(\overline{\beta}_1) = \left[\frac{\Phi(-\overline{\beta}_1)}{\lambda_H}\right]^{-b/k_1} \cdot \exp\left(\frac{k_1^2 \cdot \sigma_{\ln}^2}{2 \cdot b^2}\right) \tag{10}$$

With the Eq. 10 it is possible to define, starting from the demand $im_{\hat{D}}$, the capacity $im_{\hat{C}}$ required so that reliability index β_1 is satisfied (Eq. 7).

It is worth to note that $\gamma_{edp}(\overline{\beta}_1)$ considers a failure probability annual value. However, as previously introduced, for a construction life-cycle management reliability evaluations should regard a given t_{ref} longer than one year. Therefore, a $\gamma_{edp}(\overline{\beta})$ is required, that is the target reliability factor corresponding to $\overline{\beta}$, where $\overline{\beta}$ is the target reliability index within t_{ref}. In order to evaluate $\gamma_{edp}(\overline{\beta})$ the following formulation is proposed. As known, if the annual probability P_{f1} is constant and the events are independent, then the failure probability P_f in a certain t_{ref} may be calculated with the Eq. 11 [63]:

$$P_f = 1 - (1 - P_{f1})^{t_{ref}} \tag{11}$$

Note that $\lambda_H = 1/T_R$, and that T_R may be correlated to exceedance probability P_E of the seismic action within t_{ref} with the Poisson law (Eq. 12):

$$P_E = 1 - \exp\left(-\frac{t_{ref}}{T_R}\right) \tag{12}$$

Hence, by deriving T_R from Eq. 12 and by substituting into the Eq. 8, the Eq. 11 may be rewritten as below reported (Eq. 13):

$$P_f = 1 - \left[1 + \frac{\ln(1 - P_E)}{t_{ref} \cdot \gamma_{edp}^{k_1/b}} \cdot \exp\left(\frac{k_1^2 \cdot \sigma_{\ln}^2}{2 \cdot b^2}\right)\right]^{t_{ref}} \tag{13}$$

The Eq. 13 may be simplified as follows (Eq. 14):

$$\begin{aligned} P_f &= 1 - \left(1 + \frac{c}{t_{ref}}\right)^{t_{ref}} \cong 1 - \exp(c) \\ &= 1 - \exp\left[\frac{\ln(1 - P_E)}{\gamma_{edp}^{k_1/b}} \cdot \exp\left(\frac{k_1^2 \cdot \sigma_{\ln}^2}{2 \cdot b^2}\right)\right] \end{aligned} \tag{14}$$

In practice, for the *Serviceability Limit States* (*SLSs*) the Eq. 14 provides an acceptable approximation of Eq. 13 with an error of less than 3 % for t_{ref} higher than 10 years, and for c values that are usual for the problem under consideration. Whereas, for the *Ultimate Limit States* (*ULSs*) the error is practically negligible for any value of t_{ref}.

Therefore, by turning the Eq. 14, the following expression of *the target reliability factor* $\gamma_{edp}(\overline{\beta})$ is obtained (Eq. 15):

$$\gamma_{edp}(\overline{\beta}) = \left\{\frac{\ln[1 - \Phi(-\overline{\beta})]}{\ln(1 - P_E)}\right\}^{-b/k_1} \cdot \exp\left(\frac{k_1 \cdot \sigma_{\ln}^2}{2 \cdot b}\right) \tag{15}$$

where $P_f = \Phi(-\overline{\beta})$ and $\overline{\beta}$ is the target reliability index for a t_{ref} greater than one year.

Moreover, it is proposed to introduce the *overstrength factor* γ_0 in order to take into account the construction overstrength assumed because of the partial factors. Consequently, the *target reliability factor* $\gamma'_{edp}(\overline{\beta})$ may be calculated as follows:

$$\gamma'_{edp}(\overline{\beta}) = \frac{\gamma_{edp}(\overline{\beta})}{\gamma_0} \tag{16}$$

The notation $\gamma'_{edp}(\overline{\beta})$ is adopted for highlighting that, in this way, the overstrength influence on the structural reliability is taken into account. If mean values of material strengths are instead used then γ_0 may be assumed equal to 1.

Fig. 3 gives an example on how it is possible to define the reliability-targeted design spectrum, that is the capacity spectrum satisfying a certain reliability requirement within a t_{ref}. In detail, it plots the demand spectrum (black continuous line) given by the classical *UHA*, the required capacity spectrum (red continuous line) and the reduced one by considering the overstrength (red dot line), both reliability-targeted design spectra derived with the methodology proposed (Fig. 3a). Note that the demand spectrum includes the site effects due to the subsoil type considered by standards, such as EN 1998–1 [1] and NTC-18 [3]. For completeness, also the fragility curves having the median values of the pseudo-acceleration $S_e(T_1)$ is reported, intended as *edp* in this example (Fig. 3b). T_1 refers to the first vibration period. More in detail, $S_e(T_1)_{\hat{D}}$ is known from the demand spectrum defined through the site seismic hazard and the P_E (e.g. 10 % in 50 years; [1]). Afterwards, $S_e(T_1)_{\hat{C}}$ belonging to capacity spectrum (red continuous line) may be calculated with the Eq. 7 by means of the factor $\gamma_{edp}(\overline{\beta})$ (Eq. 15). If the overstrength is considered then the capacity spectrum should be further reduced of γ_0, such that the reduced $S_e(T_1)_{\hat{C},\gamma_0}$ may be found.

As it is clear to note, the reliability-targeted capacity spectrum or, alternatively, the reliability-targeted capacity fragility curve is directly linked to the target reliability index $\overline{\beta}$ within a t_{ref}. However, currently only ASCE [47] provides a target failure probability for seismic design. In this document the mean value for the annual *Near Collapse Limit State* (*NCLS*) exceedance probability is assumed for U.S.A., equal to $P_{f1} = 2 \times 10^{-4}$ for a P_E of 2 % hazard-exceedance probability in 50 years (i.e., $\lambda_H = 0.04\%$).

Therefore, a crucial role for defining the reliability-targeted capacity spectrum is played by $\overline{\beta}$ for each *LS* considered within a t_{ref}. The target reliability index $\overline{\beta}$ can be achieved through different design approaches. As for the limited ductility design, it is primarily based on strength, while dissipative design exploits inelastic deformations. When partial factors are used, the overstrength factor γ_0 reduces the capacity spectrum to take into account material design strengths, since the reliability-based capacity spectrum refers instead to the mean values. In addition, in the case of dissipative structural designs a further spectrum reduction is gained through the behavior factor q [3]. Both design approaches aim to ensure the same reliability.

Starting from these premises, in the next sections a procedure to calibrate the target reliability indexes for seismic designing is proposed, extended to all *LSs*. Then, an application to the Italian territory is shown, according to the current Italian standards NTC-18 [3].

3. Seismic reliability of constructions designed according to Italian standards

Nowadays, several modern design codes, such as Italian standards [3] or Eurocode [1], define seismic actions for constructions by adopting a *UHA* for the national territory. This means that the seismic hazard maps are provided for several return periods T_R considering as *IM* the *Peak Ground Acceleration* (*PGA*) or other spectral acceleration. More specifically, the Italian standards provide the *PGA* on rigid soil (a_g) together with spectral accelerations at n. 10 periods T ranging from

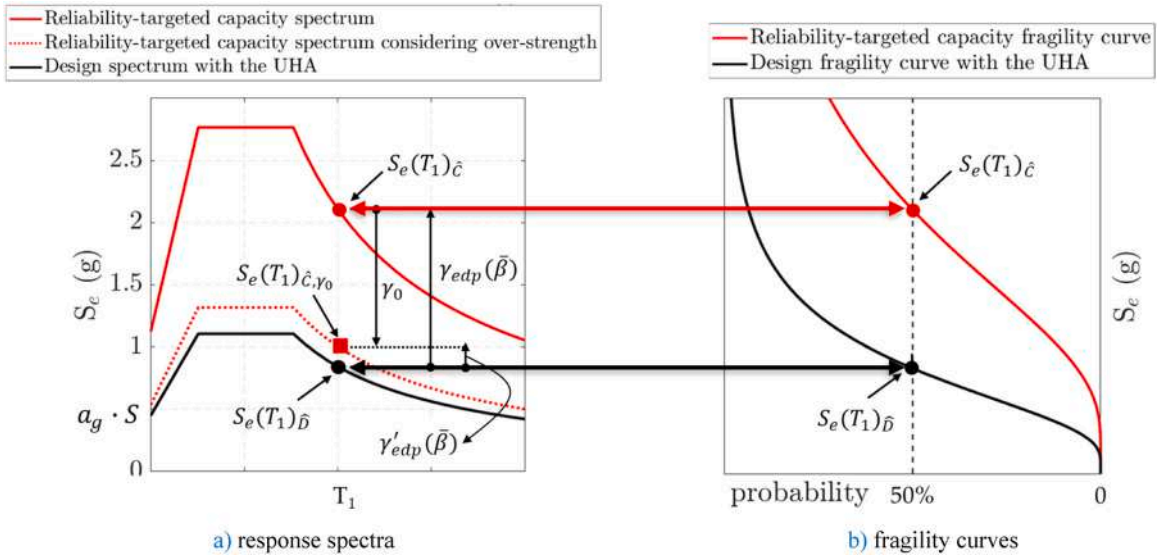

Fig. 3. Derivation of reliability-targeted design spectrum from uniform-hazard demand spectrum: a) response spectra showing demand ($S_e(T_1)_{\hat{D}}$), required capacity ($S_e(T_1)_{\hat{C}}$), and overstrength-reduced capacity ($S_e(T_1)_{\hat{C},\gamma_0}$); b) corresponding fragility curves with median values.

0.1 sec to 2.0 sec, thus enabling a detailed characterization of the hazard response spectrum.

Then, a set of principles and rules for designing must be respected so that the construction, for each *LS* considered, implicitly complies the corresponding reliability requirements.

However, by following a *UHA* the designed construction very often provides non-uniform reliability performance depending on the site seismic hazard. This becomes clear if one derives the reliability index

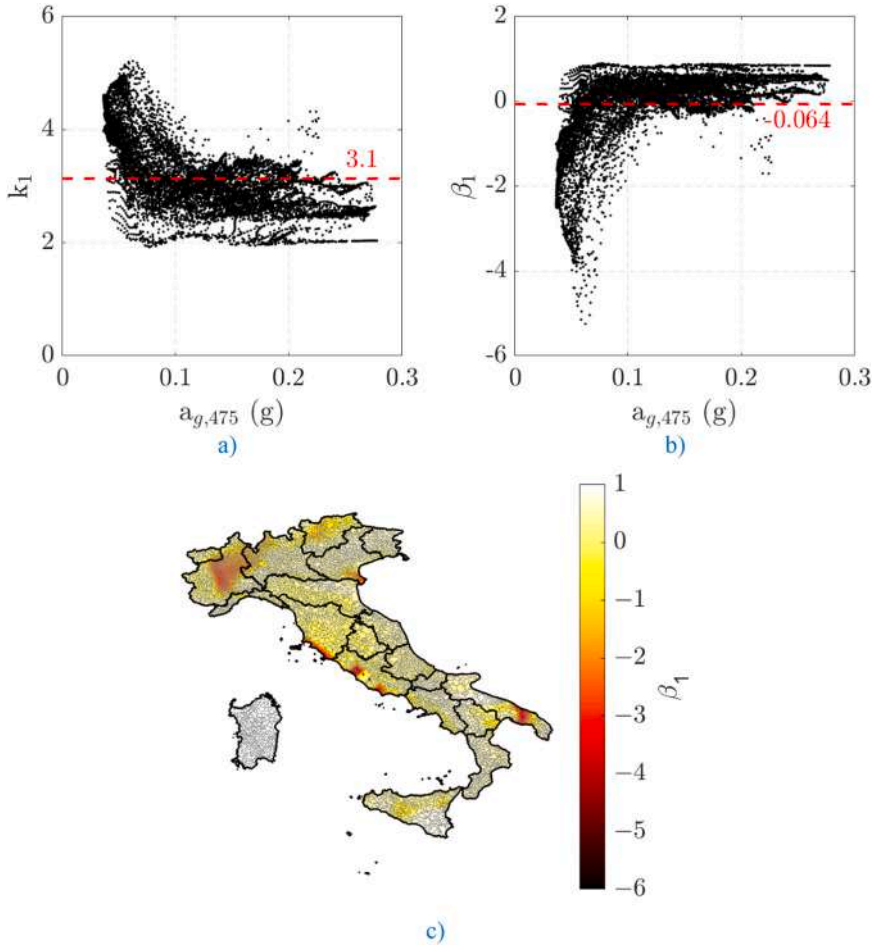

Fig. 4. Seismic reliability assessment under current UHA for $T_R = 475$ years across Italian territory: a) seismic hazard slope parameter k_1 sorted by $a_{g,475}$; b) resulting annual reliability index β_1 sorted by $a_{g,475}$; c) maps of β_1.

$\beta_1 = -\Phi^{-1}(P_{f1})$ (Eq. 8) across the Italian territory considering, for instance, $T_R = 475$ years and the values provided by the *MPS-04* hazard model, proposed by *INGV* (http://esse1.mi.ingv.it/, [60]). In this example, the parameters of the capacity fragility curves are assumed equal to $\sigma_{\ln} = 0.6$, $b = 1$ and $\gamma_{edp} = 1$. Moreover, as suggested in FEMA [10], (Eq. 3) is derived by considering the values of seismic hazard having the exceedance probabilities of 2 % and 10 % in 50 years, as follows (Eq. 17):

$$k_1 = \frac{\ln\left(\frac{\lambda_{H,475}}{\lambda_{H,2475}}\right)}{\ln\left(\frac{S_{e,475}}{S_{e,2475}}\right)} = \frac{1.65}{\ln\left(\frac{S_{e,475}}{S_{e,2475}}\right)} \tag{17}$$

where $S_{e,2475}$ and $S_{e,475}$ are the spectral pseudo-accelerations and $\lambda_{H,2475}$ and $\lambda_{H,475}$ the corresponding annual exceedance probabilities, referring to a T_R of 475 and 2475 years, respectively.

Fig. 4a plots the k_1 values obtained for all the grid points of the Italian national territory (10751 points), each of these sorted by its $a_{g,475}$, that is the seismic horizontal acceleration associated to $T_R = 475$ years. $a_{g,475}$ is assumed as representative parameter of the seismic hazard of each grid point examined. Whereas Fig. 4b shows the resulting reliability index β_1 sorted by the corresponding $a_{g,475}$. As one may easily note, β_1 is strictly dependent on the seismic hazard site, ranging between about −6 and 1, with an average value over the national territory of −0.064. The lowest values of the reliability index are obtained for seismic hazard with $a_{g,475} < 0.1g$. For completeness, Fig. 4c plots the so derived β_1 map, confirming the pronounced variability across the national territory for the chosen T_R. This result may be extended for all the values of T_R considered in the seismic hazard law.

Looking at the Fig. 4 it is easy to note that if the $a_{g,475}$ is different then, consequently, also β_1 is different. However, β_1 is still different even if the seismic design acceleration $a_{g,475}$ is equal in two different sites. As proof of this, Fig. 5 shows the hazard curves of two different sites of the Italian territory, named *Site 1* (blue line) and *Site 2* (magenta line), having the same $a_{g,475} = 0.2g$. This means that the capacity fragility curve (red continuous line) is the same for both the sites considered. Despite this, the annual failure probability P_{f1} results differently, since the two sites have a different value of k_1. In this case, $k_1 = 2.60$ for *Site* 1 and $k_1 = 3.11$ for *Site* 2, providing, respectively, $P_{f1} = 7.1 \times 10^{-3}$ and $P_{f1} = 1.2 \times 10^{-2}$ (Eq. 8). This result highlights that the reliability of constructions designed using the *UHA* varies site-by-site, even when the seismic design acceleration is the same. This is because the seismic hazard characteristics differ across national territory.

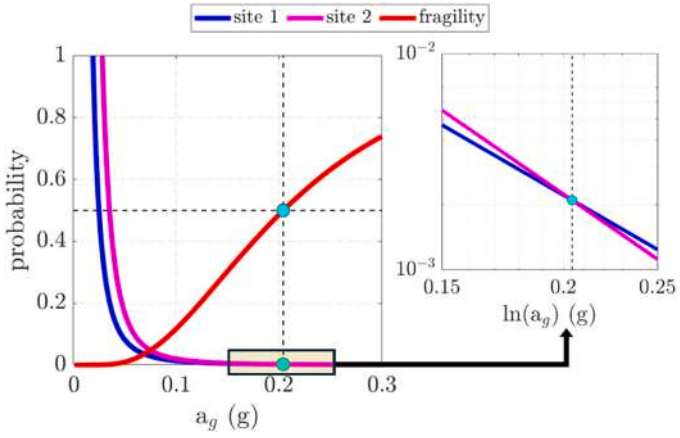

Fig. 5. Demonstration of non-uniform reliability under UHA: comparison of two Italian sites with identical design acceleration ($a_{g,475} = 0.2$ g) with different seismic hazard curves ($k_1 = 2.60$ vs $k_1 = 3.11$) resulting in different annual failure probabilities ($P_{f1} = 7.1 \times 10^{-3}$ vs $P_{f1} = 1.2 \times 10^{-2}$) for the same capacity fragility curve.

4. Derivation of seismic target reliability indexes: an application to Italian territory

In this section seismic target reliability indexes are derived, based on the *MPS-04* hazard model [60] adopted by the Italian standards NTC-18 [3]. To this scope, the following parameters influencing seismic reliability are discussed.

4.1. Exceedance probability of the seismic action

In general, performance-based standards define seismic action as function of a *LS*, with an implicit acceptable failure probability. The latter takes into account the consequences of structural failure such as, among the others, human casualties, economic losses and environmental damage.

In order to derive seismic action as function of both *LS* and *CC*, it is necessary to define the exceedance probability $P_{E,LS,CC}$ in a given t_{ref}. Then, the return period $T_{R,LS,CC}$ may be obtained with the Eq. 18:

$$T_{R,LS,CC} = -\frac{t_{ref}}{\ln(1 - P_{E,LS,CC})} \tag{18}$$

where the notation $T_{R,LS,CC}$ and $P_{E,LS,CC}$ is adopted to explicitly report their dependance on *LS* and *CC*.

It is worth to note that the $P_{E,LS,CC}$ is unknown and it may be derived, in the case of Italian standards [3], by defining a correspondence between the *Use Classes* (*UCs*) and *CCs*. In particular, the Italian standards [3] define four *Use Classes* (*UCs*) ranging from *I* to *IV*, with a specific *Coefficient of Use* C_U (Table 1), increasing as the *UC* increases. The *UC* is defined considering the construction failure consequences, depending on human lives number involved, social and environmental impact.

According to the NTC-18 [3], the return period $T_{R,LS,UC}$ may be calculated with the well-known Poisson law by means of the following relationship (Eq. 19):

$$T_{R,LS,UC} = -\frac{V_R}{\ln(1 - P_{E,LS})} = -\frac{C_U \cdot t_{ref}}{\ln(1 - P_{E,LS})} \tag{19}$$

where $P_{E,LS}$ is the exceedance probability known for all *LSs*, which include *ULSs* and *SLSs* (Table 2). The *ULSs* include *Collapse Prevention Limit State* (*CPLS*) and *Life-Safety Limit State* (*LSLS*), while the *SLSs* include *Damage Limit State* (*DLS*) and *Operational Limit State* (*OLS*). Note that the notation $T_{R,LS,UC}$ is adopted to explicitly highlight its dependance on *LS* and *UC*, and that $P_{E,LS}$ is independent on *UC*.

By equating the Eq. 18 with the Eq. 19, it is possible to derive the following relationship (Eq. 20):

$$P_{E,LS,CC} = 1 - (1 - P_{E,LS})^{1/C_U} \tag{20}$$

providing the relationship between $P_{E,LS}$ (Table 2) given by the NTC-18 [3] and the $P_{E,LS,CC}$ depending also on the *CC*. It is worth to note that the Eq. 20 is independent on t_{ref}. The Table 3 reports the correspondence adopted between *UC* and *CC* and the so derived $P_{E,LS,CC}$ values.

4.2. Logarithm standard deviation of fragility curves

In order to apply a seismic reliability-based approach, the value of the fragility curve logarithmic standard deviation $\sigma_{\ln,LS}$ has to be assumed (Eq. 13). As known, it represents the fragility curve shape

Table 1
Coefficient of Use (C_U) for different Use Classes (UCs) according to [3].

UC	*I*	*II*	*III*	*IV*
C_U	0.7	1.0	1.5	2.0

Table 2
Seismic action exceedance probability $P_{E,LS}$ for different LS in a 50-year reference period by [3].

LS	*SLS*		*ULS*	
	OLS	*DLS*	*LSLS*	*CPLS*
$P_{E,LS}$	81 %	63 %	10 %	5 %

Table 3
Seismic action exceedance probability $P_{E,LS,CC}$ as function of *LS* and *CC* as function of *Use Classes*.

$P_{E,LS,CC}$	*Use Class (UC)*			
	I	*II*	*III*	*IV*
	Consequence Class (CC) - Consequence of failure			
LS	*CC1* (Small)	*CC2* (Some)	*CC3* (Moderate)	*CC4* (Great)
OLS	86 %	81 %	73 %	66 %
DLS	72 %	63 %	50 %	40 %
LSLS	20 %	10 %	3 %	1 %
CPLS	12 %	5 %	1 %	0.3 %

providing the dispersion around the median value of the *IM* considered.

In particular, $\sigma_{\ln}$ takes into account randomness and epistemic uncertainties. The former are related to the variability associated with frequencies content and other attributes of the ground motion and refers to a given intensity measure [65]. The latter are linked to structural modeling and analysis [65].

The random uncertainties dispersion may be computed as a result of non-linear dynamic analysis (e.g. *IDA*; [27]). While, as far as the epistemic uncertainties dispersion is concerned, default values in practical applications may be used, based on statistical studies of typical structural systems [34].

The measure of the dispersion of both randomness and epistemic uncertainties are combined by means of the *Square Root of the Sum of the Squares* (*SRSS*), with the following combination rule (Eq. 21, [11]):

$$\sigma_{\ln} = \sqrt{\left(\sigma_{\ln,R}\right)^2 + \left(\sigma_{\ln,U}\right)^2} \tag{21}$$

where $\sigma_{\ln,R}$ and $\sigma_{\ln,U}$ are the measures of the *IM* logarithm standard deviation for randomness (*R*) and epistemic (*U*) uncertainties, respectively.

A similar approach is adopted in the methodology presented in FEMA P-695 [65], where a detailed procedure to quantify the *IM* logarithm standard deviation is provided. In particular, $\sigma_{\ln,R}$ may be assumed equal to 0.40 for constructions presenting a ductility μ greater, or equal, than 3. Otherwise, in the case of limited ductility, the following expression (Eq. 22) is proposed by FEMA P-695 [65]:

$$\sigma_{\ln,R} = 0.10 + 0.10 \cdot \mu \leq 0.40 \tag{22}$$

where μ is the construction ductility.

Similarly, in Dolšek & Fajfar [66] and Vamvatsikos & Fragiadakis [67] a value of $\sigma_{\ln,R}$ for the collapse limit state ranging from 0.30 to 0.45 is reported.

Therefore, in this study, coherently with the values proposed in literature, a $\sigma_{\ln,R,ULS} = 0.40$ for the *ULSs* (*LSLS, CPLS*) is assumed, and equal to $\sigma_{\ln,R,SLS} = 0.20$ for *SLSs* (*OLS, DLS*). These values correspond to the upper (0.40) and the lower bound (0.20) of Eq. 22, since $\mu = 3.0$ for *ULSs* and $\mu = 1.0$ for *SLSs* (elastic behavior) are assumed [65].

As for $\sigma_{\ln,U}$, it is quantified in FEMA P-695 [65] by means of *SRSS* rule, applied to three different dispersion measures, such as: test-data uncertainty, modeling uncertainty and design requirements uncertainty. The values of these three dispersion measures vary in the interval 0.10–0.50, and they are dependent on accuracy, robustness and confidence of the results. The resulting $\sigma_{\ln,U}$ for *ULSs* may range from 0.17 to 0.87. However, in different studies a single value of $\sigma_{\ln,U}$ is proposed. For instance, for the collapse threshold in Zareian et al. [68] and Liel et al. [69] the values of 0.40 and 0.45 are proposed, respectively.

Based on what is reported in the literature, in this study the value $\sigma_{\ln,U,ULS} = 0.45$ for *ULSs* is assumed. It should be noted that any numerical model is inherently affected by epistemic uncertainties related to modeling assumptions, material constitutive laws, and numerical discretization. Recent studies on reinforced concrete systems under cyclic loading have demonstrated that resistance model uncertainty can significantly influence structural response predictions and, consequently, fragility assessment [70].

Therefore, by applying the Eq. 21, $\sigma_{\ln,ULS} = 0.60$ is obtained, corresponding to the same value assumed in other works, such as in Fajfar & Dolšek [34]. As for the *SLS*, to date no reference for $\sigma_{\ln,U}$ is available in literature. Therefore, as suggested in Baltzopoulos et al. [30], in order to fill this gap, it may be assumed that the epistemic uncertainty propagates along the *IDA* curves in a manner ensuring their monotonicity. Consequently, the value $\sigma_{\ln,SLS} = 0.25$ is assumed to respect this trend.

For sake of completeness, the values of $\sigma_{\ln,R}$, $\sigma_{\ln,U}$ and $\sigma_{\ln}$ (Eq. 21) are summarized in Table 4, where the subscript *LS* is adopted for making explicit their dependance on *LS*.

It should be noted that the values adopted in Table 4 represent average parameters suitable for a wide variety of structural typologies commonly found in Italian construction practice. Different structural systems (e.g., reinforced concrete moment-resisting frames, masonry buildings, steel structures) may exhibit different fragility characteristics, with $\sigma_{\ln}$ values depending on structural regularity, non-linear response, design approach, and material properties. The values adopted herein are consistent with those widely used in probabilistic seismic assessment frameworks (e.g. [34,65,67]) and, therefore, may be considered a reasonable reference for establishing target reliability indexes over a national territory.

4.3. Target reliability factor

As discussed in the Sect. 2, the target reliability factor $\gamma_{edp}(\overline{\beta})$ is introduced for modifying the median value of the demand fragility curve $im_{\hat{D}}$, so that a median value of the capacity fragility curve $im_{\hat{C}}$ is found satisfying a given reliability index $\overline{\beta}$.

However, alternatively to the formulation proposed in this paper (Eq. 15) that is aligned with the approximated one proposed in FEMA [10] and Cornell et al. [11], if the failure probability is known then $\gamma_{edp}(\overline{\beta})$ may be derived directly from the convolution integral (Eq. 1). For instance, this may be done by considering the value of $\overline{P}_{f1,NCLS,CC2} = 2 \times 10^{-4}$, proposed in ASCE [47] a $P_E = 2$ % of hazard-exceedance probability in 50 years for U.S.A. (i.e. $\lambda_H = 0.04\%$). In this case it results that $\overline{\beta}_{1,NCLS,CC2} = -\Phi^{-1}\left(\overline{P}_{f1,NCLS,CC2}\right) = 3.54$. The notation $\overline{P}_{f1,NCLS,CC2}$ is adopted since it represents a target annual failure probability indicated for *NCLS* and for *CC2*. It is worth noting that this is the only value declared in ASCE [47]. For other *LSs* and *CCs* no indication is found in this document or in the published literature. Therefore, starting from the convolution integral (Eq. 1), if $\overline{P}_{f1,NCLS,CC2}$, $\lambda_H(im)$, and the fragility curve (by means of $\sigma_{\ln,ULS}$ and $im_{\hat{D}}$) are known, the target reliability factor $\gamma_{edp}\left(\overline{\beta}_{1,NCLS,CC2}\right)$ may be derived. The $\gamma_{edp}\left(\overline{\beta}_{1,NCLS,CC2}\right)$ is iteratively found by varying $im_{\hat{C}}$ starting from the $im_{\hat{D}}$ known (from the *UHA*), so that the

Table 4
Logarithmic standard deviations for fragility curves: randomness ($\sigma_{\ln,R}$), epistemic uncertainty ($\sigma_{\ln,U}$), and total combined uncertainty ($\sigma_{\ln}$) for *SLS* and *ULS*.

LS	$\sigma_{ln,R}$	$\sigma_{ln,U}$	σ_{ln}
OLS, DLS	0.20	0.25	0.32
LSLS, CPLS	0.40	0.45	0.60

$\overline{P}_{f1,NCLS,CC2}$ is guaranteed. For sake of completeness, Fig. 6 shows schematically the procedure adopted to obtain $\gamma_{edp}(\overline{\beta}_{1,NCLS,CC2})$.

$\gamma_{edp}(\overline{\beta}_{1,NCLS,CC2})$ is here calculated considering the seismic hazard function $\lambda_H(im)$ proposed in Bradley et al. [15], where the seismic hazard data are approximated with a hyperbola shape since, typically, the data have a concave downward global shape in a log-log space. This formulation is more complex than the one proposed in Sewell, Toro, & McGuire [12], and recalled in the Eq. 3, where instead a linear function in a log-log plane is adopted. The Bradley et al. [15] formulation does not suffer of the issue related to the identification of the *region of interest*, i.e. the region providing the greatest failure probability [28]. It is expressed as follows with (Eq. 23):

$$\lambda_H(im) = \lambda_{H,asy} \cdot \exp\left[\alpha \cdot \ln\left(\frac{im}{im_{asy}}\right)^{-1}\right] \tag{23}$$

where α is a constant, while $\lambda_{H,asy}$ and im_{asy} are the horizontal and vertical asymptotes, respectively.

In order to apply the Bradley et al. [15] formulation, the values of α, $\lambda_{H,asy}$ and im_{asy} are derived for each grid point of the national territory by minimizing the following *Residual Squared Sum* (*RSS*) (Eq. 24):

$$\min RSS = \sum_{i=1}^{9} \left\{\ln[\lambda_H(im_i)] - \ln\left[\lambda_{H,MPS-04}(im_i)\right]\right\}^2 \tag{24}$$

where $\lambda_{H,MPS-04}(im_i)$ is the exceedance annual rate provided by *MPS-04* hazard maps [60], and λ_H is instead the estimated one with Eq. 23.

The summation of Eq. 24 is applied to the different ground motion intensities and to all the 9 values provided in each hazard map. More in detail, this study considers the seismic hazard maps for n. 10 spectral periods T ranging between 0.1 sec and 2.0 sec, plus the peak ground acceleration a_g on rigid soil (i.e. $T = 0$), for a total of 99 seismic hazard maps. As known, for each map the im_i is provided for 9 different T_R ($i = 1, \ldots, 9$) corresponding to 9 occurrence probability P_E (Table 5), considering the ideal conditions of a rigid soil with a horizontal topographic surface (category A according to [3]).

As result of the calibration of the Bradley et al. [15] formulation, Fig. 7.a shows for each grid point the value of the resulting determination coefficient R^2 [71]. It measures the scatter between the *MPS-04* hazard law and the predicted one with the law proposed by Bradley et al. [15]. In this case a_g is chosen as *im*, and the resulting R^2 is plotted as function of $a_{g,475}$. Moreover, in Fig. 7.a the maximum and the minimum value of R^2 is highlighted, resulting equal to $R^2_{\max} = 1$ and $R^2_{\min} = 0.90329$ for the municipalities of Barcellona Pozzo di Gotto (Lat: 38.1215; Lon: 15.2024) and Fasano (Lat: 40.8154; Lon: 17.4545), respectively. For completeness, Fig. 7.b depicts the seismic hazard curves $a_g - \lambda_H$ for the these two municipalities, using both the *MPS-04* model values and the ones predicted by Bradley et al. [15]. It is easy to note that, even in the case of $R^2_{\min}$, the scatter between the seismic hazard values is really negligible.

Fig. 8 reports the values of $\gamma_{edp}(\overline{\beta}_{1,NCLS,CC2})$ for all the grid points of the Italian territory derived from the convolution integral (Fig. 6), considering the Bradley et al. [15] formulation, calibrated as previously illustrated. The values of $\gamma_{edp}(\overline{\beta}_{1,NCLS,CC2})$ are sorted as function of $a_{g,475}$, and calculated for n. 11 spectral periods T, varying from 0 to 2.0 sec. Also, in each graph the mean value and the interval defined as mean value +/− one standard deviation is reported, evaluated on the overall sample of the obtained results. As one may observe, the resulting mean values and standard deviations are really close, as demonstrated in the histogram of Fig. 9.

The values of $\gamma_{edp}(\overline{\beta}_{1,NCLS,CC2})$ obtained consent to derive capacity fragility curves for a given construction so that the $\overline{P}_{f1,NCLS,CC2}$ is uniform all-over the Italian national territory. It is noteworthy that the results here discussed are valid in this case for *NCLS* and *CC2*. In general, if the P_{f1} is known then the procedure applied in this section may be repeated for all *LSs*, such as *ULSs* or *SLSs,* and all the *CCs*. However, in literature there is a lack of information in this regard with exception, as already discussed, of *NCLS* and *CC2*. Therefore, it is assumed that for all *ULSs* and *CCs* the target reliability factor $\gamma_{edp}(\overline{\beta}_{1,ULS,CC})$ is equal to 2.11 and that, therefore, the reference seismic action ($im_{\bar{D}}$) accounts for the distinction between *LSLS* to *CPLS,* and from *CC1* to *CC4*.

Similarly, also for the *SLSs* to date no indication is available in literature for the corresponding P_{f1} for any *CC*. Therefore, in this case it is not possible, as done above for *ULSs* and for *CC2*, to evaluate the $\gamma_{edp}(\overline{\beta}_{1,SLS,CC2})$. However, this study wants to cover also this gap, providing a first tentative for defining the target reliability factor $\gamma_{edp}(\overline{\beta}_{1,SLS,CC})$, obtaining in this way a complete procedure with respect both *ULSs* and *SLSs*. To this scope, some consideration may be made in order to preliminary assume the value of $\gamma_{edp}(\overline{\beta}_{1,SLS,CC})$. Firstly, the failure probabilities for *SLSs* are usually greater than the *ULSs* ones. Moreover, generally for serviceability checks, contrary to the *ULSs*, partial factors are not usually applied to materials or loads. Consequently, in light of these considerations, in this study it is assumed $\gamma_{edp}(\overline{\beta}_{1,SLS,CC})$ equal to 1 and that, similarly to the *ULS*, the reference seismic action accounts for the variation between *DLS* to *OLS* and from *CC1* to *CC4*.

Anyway, it should be remarked that the procedure proposed in this study and, consequently, the reliability-based seismic action calibration across the Italian territory depends on the assumptions made for $\gamma_{edp}(\overline{\beta}_{1,ULS,CC})$ and $\gamma_{edp}(\overline{\beta}_{1,SLS,CC})$. Anyway, if in future different $\gamma_{edp}(\overline{\beta}_{1,ULS,CC})$ and $\gamma_{edp}(\overline{\beta}_{1,SLS,CC})$ values will be available, then the cali-

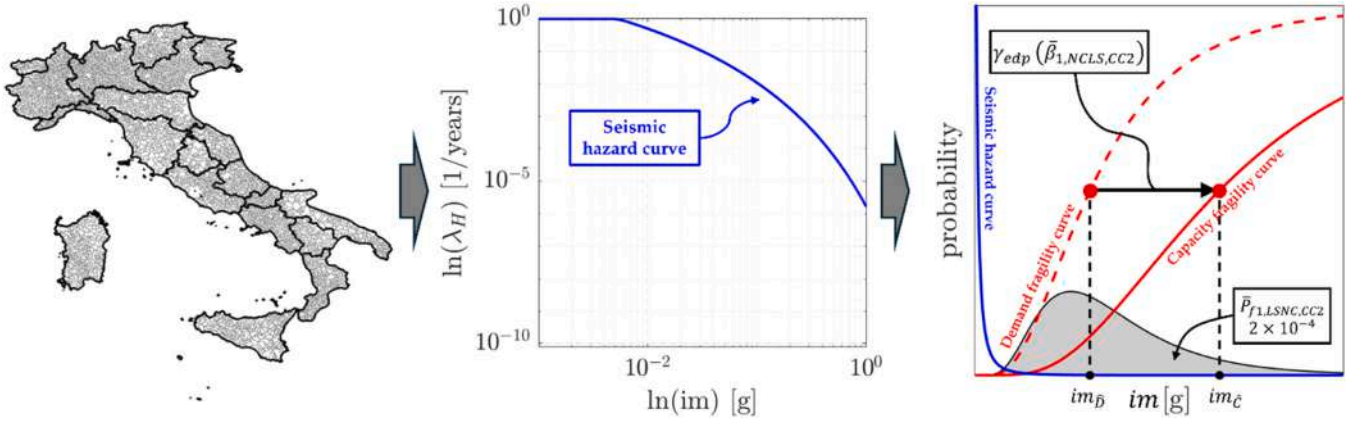

Fig. 6. Iterative procedure for deriving target reliability factor $\gamma_{edp}(\overline{\beta}_{1,NCLS,CC2})$ through convolution integral (Eq. 1) by varying capacity fragility curve median ($im_{\bar{C}}$) until target annual failure probability $\overline{P}_{f1,NCLS,CC2} = 2 \times 10^{-4}$ is satisfied.

Table 5
Return periods (T_R) and corresponding probabilities (P_E) of seismic action considered in the *MPS-04* hazard model for a reference period of 50 years.

T_R (years)	30	50	72	101	141	201	475	975	2475
P_E	81 %	63 %	50 %	39 %	30 %	22 %	10 %	5 %	2 %

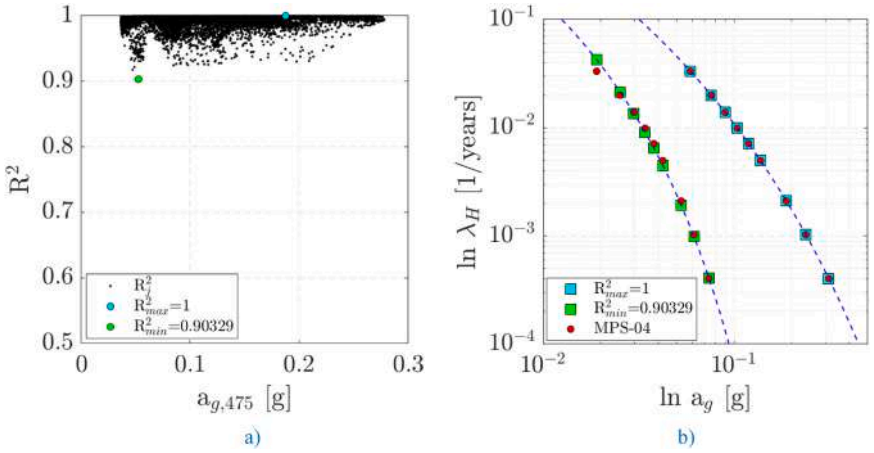

Fig. 7. Statistical validation of Bradley et al. [15] hyperbolic hazard formulation against MPS-04 data: a) coefficient of determination (R^2) for all 10751 Italian grid points sorted by $a_{g,475}$, showing $R^2_{\min} = 0.903$; b) comparison of hazard curves for sites with maximum (Barcellona Pozzo di Gotto) and minimum (Fasano) R^2 values.

bration may be repeated for taking into the account these specific values that, to date, are not yet available within the scientific literature.

4.4. Seismic hazard function calibration

The annual failure probability P_{f1} calculated with the closed form of the Eq. 5 [11] considers the Sewell, Toro, & McGuire [12] (Eq. 3) formulation for the seismic hazard function $\lambda_H(im)$, expressed with a linear function in log-log plane through the constants k_0 and k_1. In order to accurately calibrate these constants for the Italian territory the following procedure is adopted, considering a_g as *IM*.

Firstly, it should be noted that the Eq. 3 may provide a reasonable estimate of the seismic hazard only in the range of exceedance annual rate $\lambda_H(im)$ where the failure probability is maximized (i.e. *region of interest*) [28]. To this scope, to date several methods are proposed. For instance, as also discussed in Sect. 4, the seismic hazard function may be fitted through two points having, respectively, 10 % (i.e. design basis earthquake) and 2 % (maximum considered earthquake) of exceedance in 50 years [10].

As regards k_0, it is necessary to know at least one value of *IM* corresponding to a T_R. It may be typically obtained from the seismic hazard map, which is applied to a given probability of ground motion exceedance (e.g., 10 % in 50 years) or, alternatively, to a given T_R (e.g. 475 years).

As example, Fig. 10 compares in a log-log plane for L'Aquila site the seismic hazard data given by the *MPS-04* hazard map in terms of a_g (*PGA* on a rigid soil, red squares) and the predicted ones obtained with the Eq. 3 (black line). The latter are derived according to FEMA [10] formulation (Eq. 17), resulting in this case equal to $k_0 = 3.75 \times 10^{-5}$ $(g \bullet years)^{-1}$ and $k_1 = 2.99$.

One may easily note that since the hazard data has a concave downward shape the predicted linear function overestimates the exceedance annual rate λ_H starting from $1/T_R = 0.0021 = 1/475$ years^{-1}. Therefore, in order to better fit over the entire λ_H interval the seismic hazard data, a numerical analysis is performed to obtain the values of k_0 and k_1 by minimizing the differences between the failure probability obtained with the power law expression proposed by Sewell, Toro, & McGuire [12] (Eq. 3) and the one calculated with the Bradley et al. [15] formulation (Eq. 23). As discussed in the previous section, the more complex formulation of Bradley et al. [15] (Eq. 23) has been calibrated in this study for all the Italian territory grid points for calculating the failure probability with the convolution integral (Eq. 1).

According to FEMA [10], the expression for the k_1 (Eq. 3) may be generalized as follows (Eq. 25):

$$k_1 = \ln\left(\frac{\lambda_{H,r}}{\lambda_{H,c}}\right) \cdot \left[\ln\left(\frac{im_r}{im_c}\right)\right]^{-1} \tag{25}$$

where the couples $(\lambda_{H,r}; im_r)$ and $(\lambda_{H,c}; im_c)$ refer to the *r-th* and *c-th* seismic hazard data considered for the linearization in the log-log plane. As known, for the Italian territory the *MPS-04* hazard model [60] provides the seismic hazard data for 9 different T_R ($1/\lambda_H$, Table 5). In this study, all the possible combinations of the couples are examined for the linearization in the log-log plane and for calibrating, consequently, in each grid point k_0 (Eq. 3) and k_1 (Eq. 25). In total, 36 combinations of couples are obtained and indicated in Table 6, where each dot identifies a couple made by the $(\lambda_{H,r}; im_r)$ and $(\lambda_{H,c}; im_c)$ data, briefly indicated as couple *rc* (*r-th* raw and *c-th* column).

For each couple *rc* the following objective function $f^{rc}()$ (Eq. 26) is assumed over all the national territory grid points (10751points), and extended to all *LSs* and *CCs*:

$$f^{rc}\left(k_0, k_1, \gamma_{edp}\right) = \sum_{LS}\sum_{CC}[(\bar{r}-1) + \sigma_{\bar{r}}] \tag{26}$$

where $\bar{r}$ and $\sigma_{\bar{r}}$ are mean and standard deviation of all the ratios r_i, given by the following (Eq. 27):

$$r_i = \frac{P_{f1,LS,CC,i}}{\widehat{P}_{f1,LS,CC,i}} \; with \; i = 1, \quad \ldots, \quad 10751 \tag{27}$$

$P_{f1,LS,CC,i}$ is the annual failure probability considering the couple *rc* and obtained with seismic hazard curve of Sewell, Toro, & McGuire [12] (Eq. 3), where k_1 and k_0 are calculated point-by- point in the national grid with the Eq. 25 and Eq. 3, respectively; while $\widehat{P}_{f1,LS,CC,i}$ is the annual failure probability assumed as reference for calibrating k_1 and k_0, and calculated considering the Bradley et al. [15] seismic hazard law (Eq. 23), whose parameters have been calibrated in the previous section. In

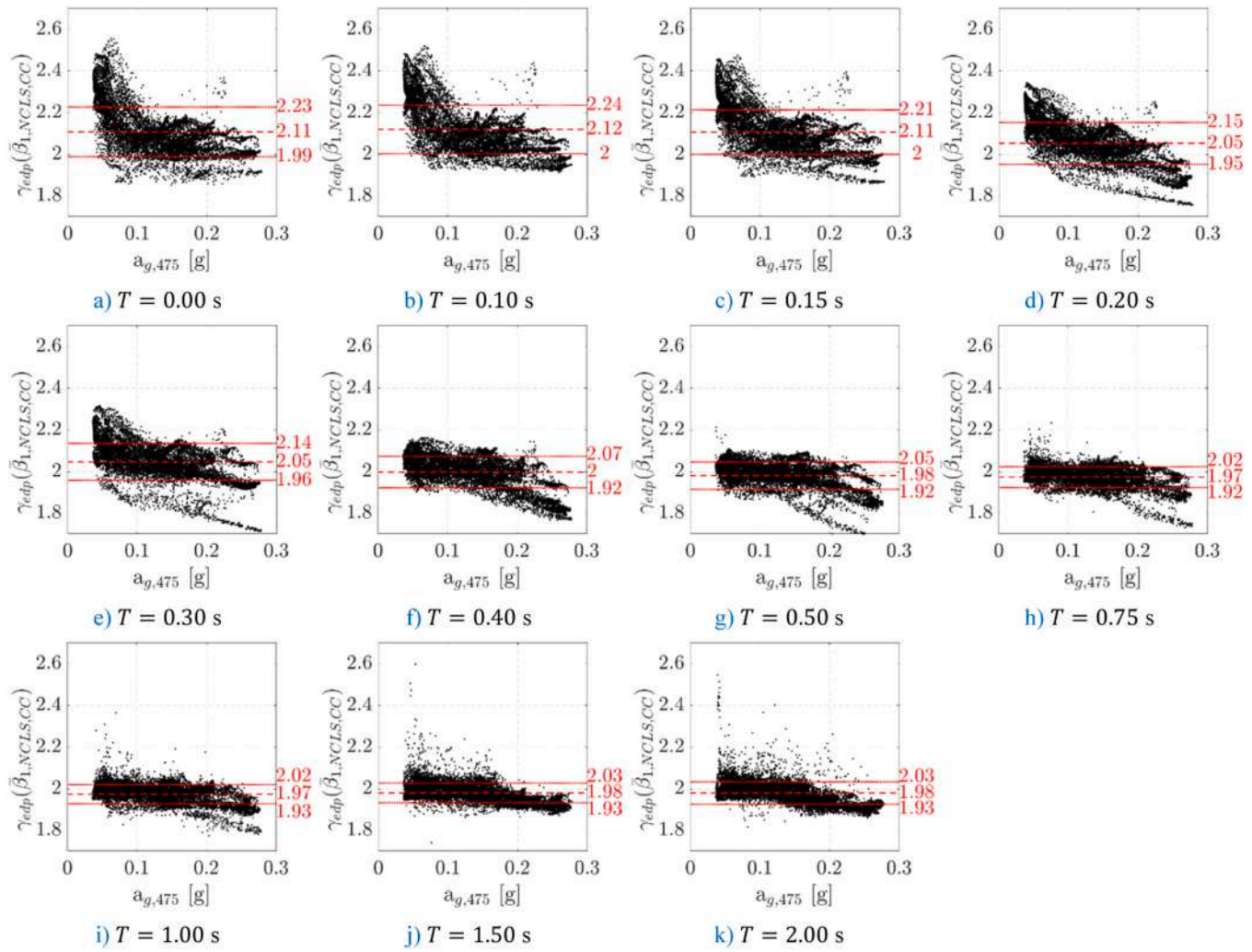

Fig. 8. Target reliability factors $\gamma_{edp}(\overline{\beta}_{1,NCLS,CC2})$ derived from convolution integral for NCLS and CC2 across all Italian grid points as function of $a_{g,475}$, for spectral periods ranging from $T = 0$ (*PGA*) to $T = 2.0$ s. Mean values and ±1 standard deviation intervals are shown.

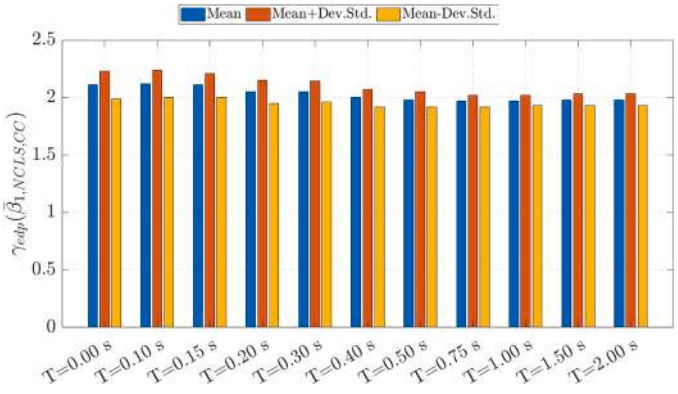

Fig. 9. Target reliability factors across spectral periods: mean values and standard deviation intervals of $\gamma_{edp}(\overline{\beta}_{1,NCLS,CC2})$ for $T = 0$–2.0 s.

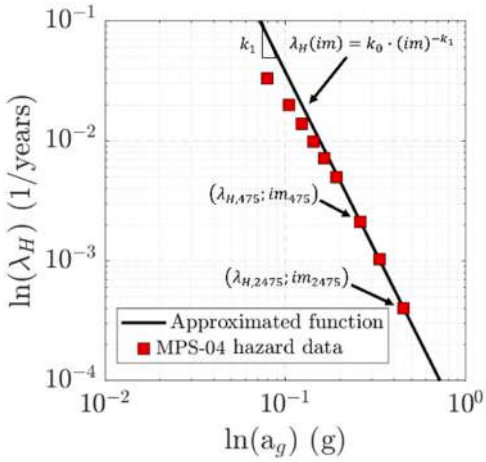

Fig. 10. Limitations of linear power-law approximation [12] for L'Aquila site: comparison between MPS-04 hazard data (red squares) and predicted values using FEMA 350 approach (black line).

the objective function $f^{rc}()$ both $P_{f1,LS,CC,i}$ and $\widehat{P}_{f1,LS,CC,i}$ are calculated with the convolution integral (Eq. 1). If $f^{rc}()$ is close to zero then the pair (k_0, k_1) permits to estimate the annual failure probability close to the one obtained considering the Bradley et al. [15] formulation (Eq. 23). In the Eq. 27 the parameters assumed are: $\sigma_{\ln,ULS} = 0.6$, $\gamma_{edp,ULS} = 2.11$, $\sigma_{\ln,SLS} = 0.32$, $\gamma_{edp,SLS} = 1$, and $b = 1$.

The objective function $f^{rc}()$ is designed to simultaneously minimize both systematic bias, through the term $(\bar{r}-1)$, and random scatter through $\sigma_{\bar{r}}$ in the prediction of failure probabilities. This dual criterion

Table 6
Matrix of 36 hazard data couples (return period combinations) evaluated for optimizing the power-law seismic hazard function parameters k_0 and k_1.

T_R ($1/\lambda_H$)	30	50	72	101	140	201	475	975	2475
30	—	●	●	●	●	●	●	●	●
50	·	—	●	●	●	●	●	●	●
72	·	·	—	●	●	●	●	●	●
101	·	·	·	—	●	●	●	●	●
140	·	·	·	·	—	●	●	●	●
201	·	·	·	·	·	—	●	●	●
475	·	·	·	·	·	·	—	●	●
975	·	·	·	·	·	·	·	—	●
2475	·	·	·	·	·	·	·	·	—

ensures that the selected hazard curve parameters provide unbiased estimates across the entire national territory while minimizing site-to-site variability. The summation over all *LSs* and *CCs* ensures that the calibration is balanced across different performance levels, avoiding optimization that favors specific limit states at the expense of others.

Fig. 11 shows in the form of histogram the values of $f^{rc}()$ function for each of the 36 combinations of couples considered (Table 6). It is clear to observe that $f^{rc}()$ has the minimum value with the couple 30–975, that is the couple of seismic hazard data referred to $T_R = 30$ years $(\lambda_{H,30}; im_{30})$ and $T_R = 975$ years $(\lambda_{H,975}; im_{975})$ (highlighted with a red bar), respectively.

As example, Fig. 12 compares for L'Aquila site the seismic hazard function obtained with the Bradley et al. [15] formulation (Eq. 23) with the Sewell, Toro, & McGuire [12] (Eq. 3) one. For the former, as calculated in the previous section, the parameters α, $\lambda_{H,asy}$, and im_{asy} (Eq. 23) result equal to 92.62, 20219 and 83.53, respectively. For the latter, k_1 and k_0 (Eq. 25 and Eq. 3) are derived considering the couple of seismic hazard data referred to $T_R = 30$ years and $T_R = 975$ years, resulting equal to $k_1 = 2.41$ and $k_0 = 7.3 \times 10^{-5}$ $(g \bullet \text{years})^{-1}$. Whereas, Table 7 shows the annual failure probabilities $P_{f1,LS,CC,i}$ and $\widehat{P}_{f1,LS,CC,i}$ (Eq. 27) of L'Aquila site, by varying the *CCs* and the *LS*. Also, the corresponding ratio r_i (Eq. 23) is reported. It should be noted that r_i varies between 0.86 (*DLS-CC4*) and 1.5 (*CPLS- CC4*), with a mean value of 0.98 and a standard deviation of 0.15 (coefficient of variation of 0.15).

For completeness, Fig. 13 reports the interval defined as mean (square dot) plus/minus one standard deviation of the ratios r_i (Eq. 27) calculated for all the grid points of Italian territory, and for the different *LSs* and *CCs*. The ratios r_i depend on the k_0 and k_1 values computed considering the seismic hazard data couple referred to $T_R = 30$ years and

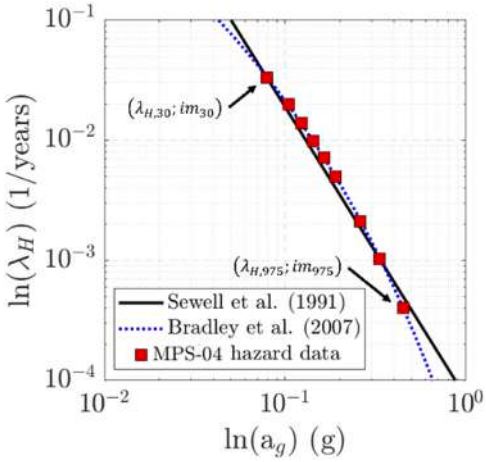

Fig. 12. Comparison of seismic hazard formulations for L'Aquila site: *MPS-04* data (red squares), Bradley et al. [15] hyperbolic model (blue line), and optimized Sewell, Toro, & McGuire [12] power-law using $T_R = 30$–975 years couple (black line, $k_1 = 2.41$).

$T_R = 975$ years. It is observed that for *SLSs* the scatter of the failure probabilities is higher than the *ULSs* ones. As already highlighted, this is due to the fact that for low values of T_R the seismic hazard curve tends to have a more marked concave downward shape and, therefore, the scatter with the Eq. 3 becomes more evident.

Finally, Fig. 14 shows the maps over the national territory of k_0 and k_1 derived considering the couple of seismic hazard data related to a T_R of 30 and 975 years. k_0 (Fig. 14.a) is ranged from 1.09×10^{-8} to around 2.27×10^{-4} $(g \bullet years)^{-1}$. Whereas, k_1 falls within the range of 1.60 to around 4.05 (Fig. 14.b).

4.5. Procedure to derive the seismic target reliability indexes

In this section, based on the assumptions made in the previous sections, seismic target reliability indexes are calibrated based on the *MPS-04* hazard model [60] adopted by the Italian standards NTC-18 [3]. They are derived considering: the target reliability factors $\gamma_{edp}(\overline{\beta}_{1,ULS,CC})$ and $\gamma_{edp}(\overline{\beta}_{1,SLS,CC})$ assumed the Sect. 0; the exceeding probability of exceedance for the seismic action indicated in the Sect. 4.1; the logarithm standard deviation of fragility curve of Sect. 4.2; and the seismic hazard

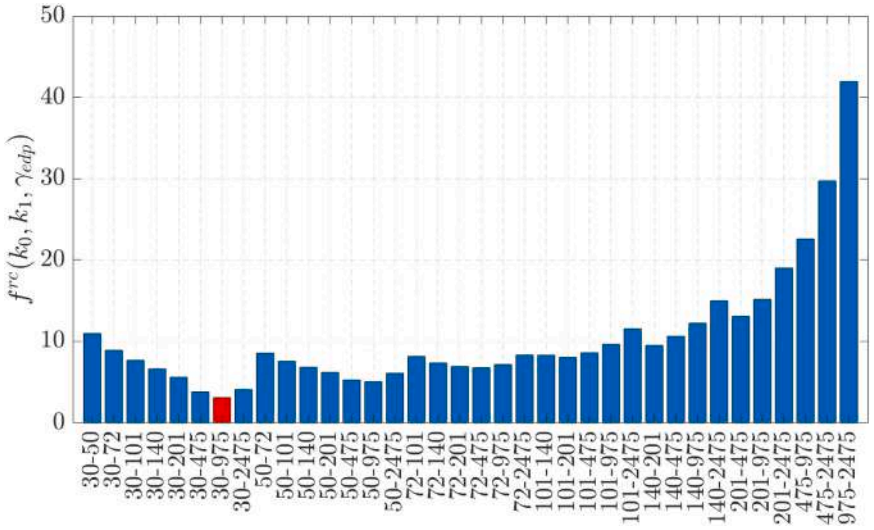

Fig. 11. Objective function $f^{rc}()$ values for all 36 return period combinations (Table 6) evaluated across the Italian territory, identifying the optimal couple $T_R = 30$–975 years (red bar) that minimizes failure probability prediction error for all *LS* and *CC*.

Table 7
Comparison of annual failure probabilities for L'Aquila site calculated using power-law ($P_{f1,LS,CC,i}$) and hyperbolic ($\widehat{P}_{f1,LS,CC,i}$) hazard formulations for different *LS* and *CC*, with resulting ratios r_i.

	OLS				***DLS***			
	***CC1* (Small)**	***CC2* (Some)**	***CC3* (Moderate)**	***CC4* (Great)**	***CC1* (Small)**	***CC2* (Some)**	***CC3* (Moderate)**	***CC4* (Great)**
$P_{f1,LS,CC,i}$	0.02	0.0199	0.0117	0.0084	0.0162	0.0102	0.0066	0.0048
$\widehat{P}_{f1,LS,CC,i}$	0.02	0.0199	0.0127	0.0095	0.0168	0.0113	0.0076	0.0056
r_i	1.00	1.00	0.92	0.88	0.96	0.90	0.87	0.86
	LSLS				***CPLS***			
	***CC1* (Small)**	***CC2* (Some)**	***CC3* (Moderate)**	***CC4* (Great)**	***CC1* (Small)**	***CC2* (Some)**	***CC3* (Moderate)**	***CC4* (Great)**
$P_{f1,LS,CC,i}$	0.0012	0.0009	0.0006	0.0005	0.0006	0.0005	0.0003	0.0003
$\widehat{P}_{f1,LS,CC,i}$	0.0013	0.0009	0.0006	0.0005	0.0007	0.0005	0.0003	0.0002
r_i	0.92	1.00	1.00	1.00	0.86	1.00	1.00	1.50

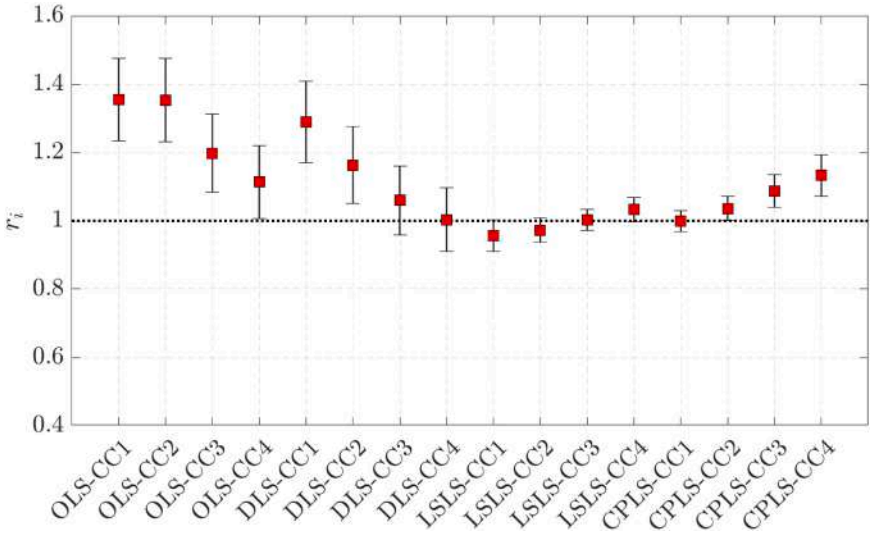

Fig. 13. Statistical validation of power-law hazard approximation: ratios r_i (Eq. 27) between failure probabilities calculated with simplified [12] and reference [15] formulations for all Italian grid points. Mean values and ±1 standard deviation intervals are shown for each *LSs* and *CCs*.

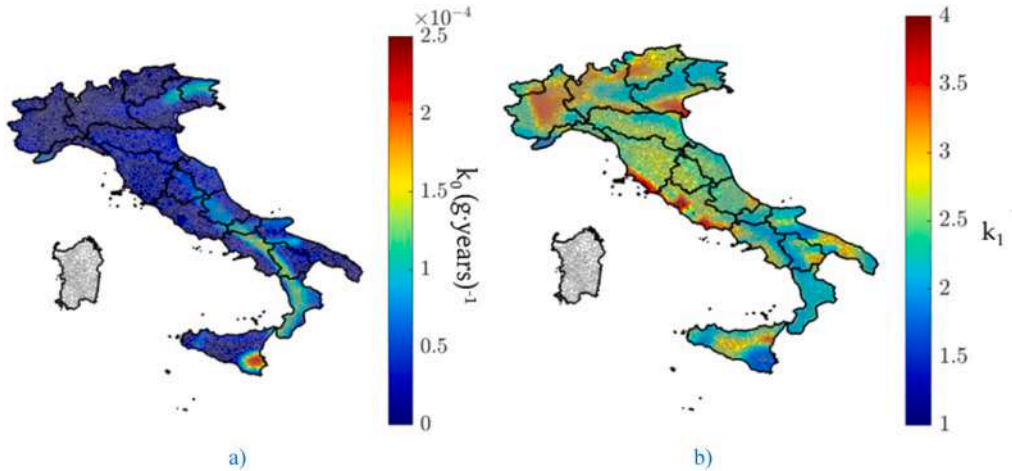

Fig. 14. Maps of calibrated power-law seismic hazard parameters over Italian territory using optimal T_R = 30–975 years couple: a) intercept k_0 (ranging from 1.09 ×10⁻⁸ to 2.27 ×10⁻⁴ g·year⁻¹); b) slope k_1 (ranging from 1.60 to 4.05).

function calibrated in the Sect. 4.4.

The resulting seismic target reliability indexes are derived with the closed form of Eq. 14, considering the a_g as *im*. Note that the failure probability P_f, and consequently the target reliability index, may be considered independent on the t_{ref} (Eq. 14) implying that $\gamma_{edp}(\overline{\beta}_{1,ULS,CC}) = \gamma_{edp}(\overline{\beta}_{ULS,CC})$ and $\gamma_{edp}(\overline{\beta}_{1,SLS,CC}) = \gamma_{edp}(\overline{\beta}_{SLS,CC})$. More in detail, for the *i-th* point of the Italian territory grid, the seismic hazard function slope k_1 is calculated (Eq. 25) with the couple of seismic hazard data referred to T_R = 30 years and T_R = 975 years. Then, $im_{\tilde{D}}$ is estimated from the related $P_{E,LS,CC}$ for a given *LS* and *CC* (Table 3). By knowing $\sigma_{\ln,LS}$ and $\gamma_{edp}(\overline{\beta}_{LS,CC})$, $P_{f,LS,CC}$ (Eq. 14) and, consequently, $\beta_{LS,CC} = \Phi^{-1}(P_{f,LS,CC})$ is calculated. Finally, the target seismic reliability index $\overline{\beta}_{LS,CC}$ of all the

National territory may be derived as mean value, or as a fractile, of the resulting $\beta_{LS,CC}$ distribution. For the sake of clarity, Fig. 15 summarizes the procedure flowchart for determining the seismic target reliability index here proposed.

As far as the *ULSs* are concerned, Fig. 16 shows the $\beta_{ULS,CC}$ values of all grid points for all the *CCs*, referring to $\gamma_{edp}(\overline{\beta}_{ULS,CC}) = 2.11$, $\sigma_{\ln,ULS} = 0.6$ and $b = 1$. In detail, they are plotted considering the *LSLS* (Fig. 16.a-d) and the *CPLS* (Fig. 16.e-h) sorted by $a_{g,475}$. In these graphs the target reliability indexes $\overline{\beta}_{ULS,CC}$ are calculated as the mean value of all the $\beta_{ULS,CC}$ values. Whereas, as regards the *SLSs*, Fig. 17 depicts the $\beta_{SLS,CC}$ values for the *OLS* (Fig. 17.a-d) and the *DLS* (Fig. 17.e-h), calculated considering $\gamma_{edp}(\overline{\beta}_{SLS,CC}) = 1$, $\sigma_{\ln,SLS} = 0.32$ and $b = 1$. One may note that in the case of Fig. 16, when $a_{g,475} > 0.1$g, the $\beta_{SLS,CC}$ values tend to stabilize around the mean value $\overline{\beta}_{SLS,CC}$. Whereas, for $a_{g,475} < 0.1$g the $\beta_{SLS,CC}$ values are more dispersed and lower than $\overline{\beta}_{SLS,CC}$. On the contrary, the Fig. 17 shows a more dispersed trend but, in any case, the $\beta_{SLS,CC}$ values reduce as $a_{g,475}$ reduces.

Finally, Table 8 and Table 9 summarize the so-derived target reliability indexes $\overline{\beta}_{LS,CC}$, indicated into the Fig. 16 and Fig. 17.

It is obvious to note that the $\overline{\beta}_{LS,CC}$ value increases from *CC1* to *CC4* and from *SLSs* to *ULSs*. The proposed value of $\overline{\beta}_{LSLS,CC2}$ equal to 1.63 (Fig. 16.b and Table 8) is consistent with the same target index proposed in Franchin & Noto [59], where the value 1.62 for $T_R = 475$ years is indicated. Furthermore, it is clear to observe that also negative values of $\overline{\beta}_{SLS,CC}$ are obtained are (Table 9), since failure probabilities greater than 50 % are obtained. It is worth noting that the exceedance probability P_E for *SLSs* adopted in the NTC-18 [3] are different from those indicated in Eurocode 8 (EC8, [1]). In particular, Eurocode provides for *DLS* $P_E = 10\%$ in 10 years ($T_R = 95$ years), while NTC-18 [3], for the same *LS*, provides $P_E = 63\%$ in 50 years ($T_R = 50$ years). $P_E = 63\%$ was derived by maintaining a ratio of 2.5 between the *DLS* and *LSLS* horizontal spectrum, also introduced in the previous OPCM 3274, [72] to differentiate severe from less severe earthquakes. However, it has been observed that by using a factor 2.5 from the *LSLS* to *DLS* horizontal spectrum a seismic action having a $T_R = 95$ years is not guaranteed overall the Italian territory. Note that also the EC8 differentiates the *DLS* seismic action. Unlike the EN 1998–1 [1], in EN 1998–3 [73] the requirement for *DLS* is associated to $P_E = 20\%$ in 50 years ($T_R = 225$ years). For this reason for completeness Table 10 summarizes also the $\overline{\beta}_{DLS,CC}$ associated to $T_R = 95$ years and $T_R = 225$ years, derived following the procedure indicated in the flowchart of Fig. 15.

5. Target reliability factors for Italian territory

In this section the target reliability factors $\gamma_{edp}(\overline{\beta}_{ULS,CC})$ and $\gamma_{edp}(\overline{\beta}_{SLS,CC})$ are calculated, through the Eq. 15, starting from $\overline{\beta}_{ULS,CC}$ and $\overline{\beta}_{SLS,CC}$ (Table 8 and Table 9, respectively) calibrated in the previous section. In this way, coherently with the reliability-based design of constructions, the reliability-targeted capacity spectrum may be defined (Fig. 3).

As example, Fig. 18a shows the resulting $\gamma_{edp}(\overline{\beta}_{ULS,CC})$ values obtained for all the grid points of the Italian territory, and correlated to $\overline{\beta}_{LSLS,CC2} = 1.63$ (green dots), where the values are sorted by $a_{g,475}$. It can be clearly observed that the values of $\gamma_{edp}(\overline{\beta}_{LSLS,CC2})$ are more dispersed when $a_{g,475} < 0.1$g, while for $a_{g,475} > 0.1$g the $\gamma_{edp}(\overline{\beta}_{LSLS,CC2})$ values tend to decrease as the $a_{g,475}$ increases. Moreover, Fig. 18a also depicts the $\gamma'_{edp}(\overline{\beta}_{LSLS,CC2})$ values (blue dots), derived by assuming a value of the overstrength factor $\gamma_0 = 2.11$ (Eq. 16). One may note that in this case the $\gamma'_{edp}(\overline{\beta}_{LSLS,CC2})$ average value calculated over the national territory is equal to 1.0. This demonstrates that if a $\gamma_0 = 2.11$ would be assumed with a *UHA* then, on average, the reliability target indexes are guaranteed and, therefore, the reliability-based approach is pursued. This result

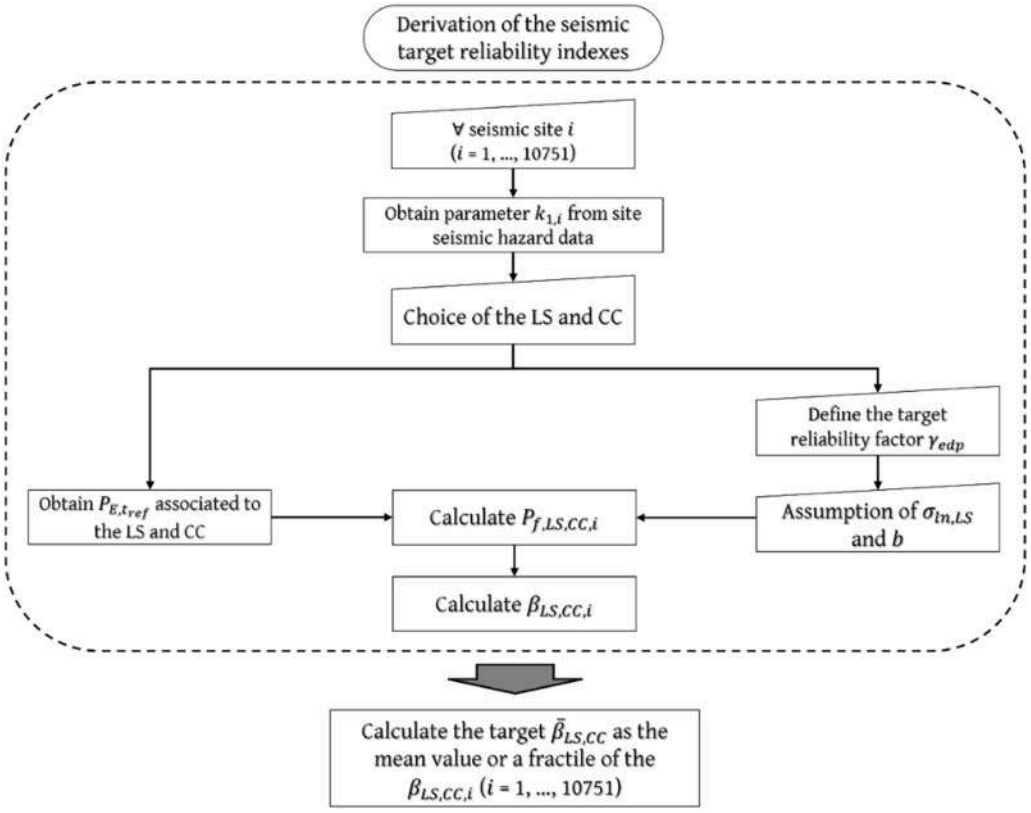

Fig. 15. Detailed flowchart for deriving target reliability indexes ($\overline{\beta}_{LS,CC}$) as function of *LS* and *CC*.

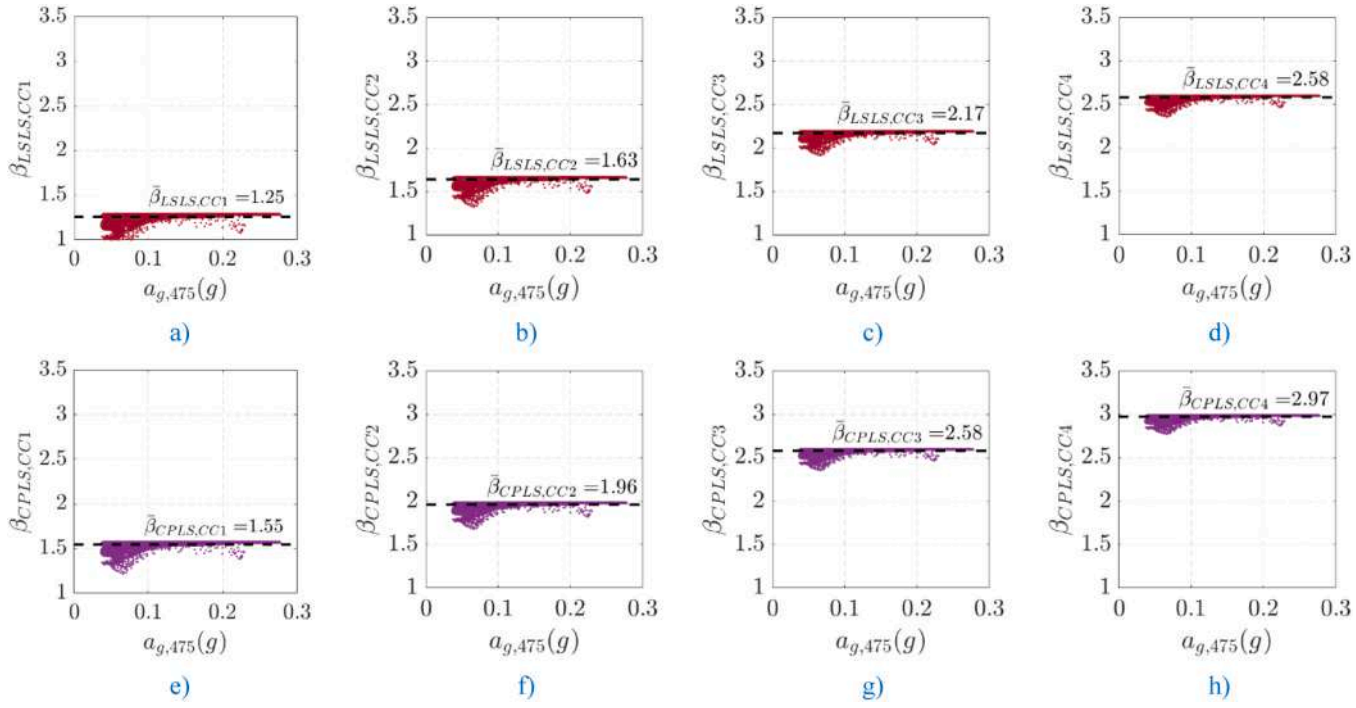

Fig. 16. Target reliability indexes for *ULS* ($\bar{\beta}_{ULS,CC}$) across Italian territory sorted by $a_{g,475}$, assuming $\gamma_{edp} = 2.11$, $\sigma_{\ln,ULS} = 0.6$, and $b = 1$: a-d) *LSLS* for *CC1-CC4*; e-h) *CPLS* for *CC1-CC4*. Horizontal lines indicate mean values.

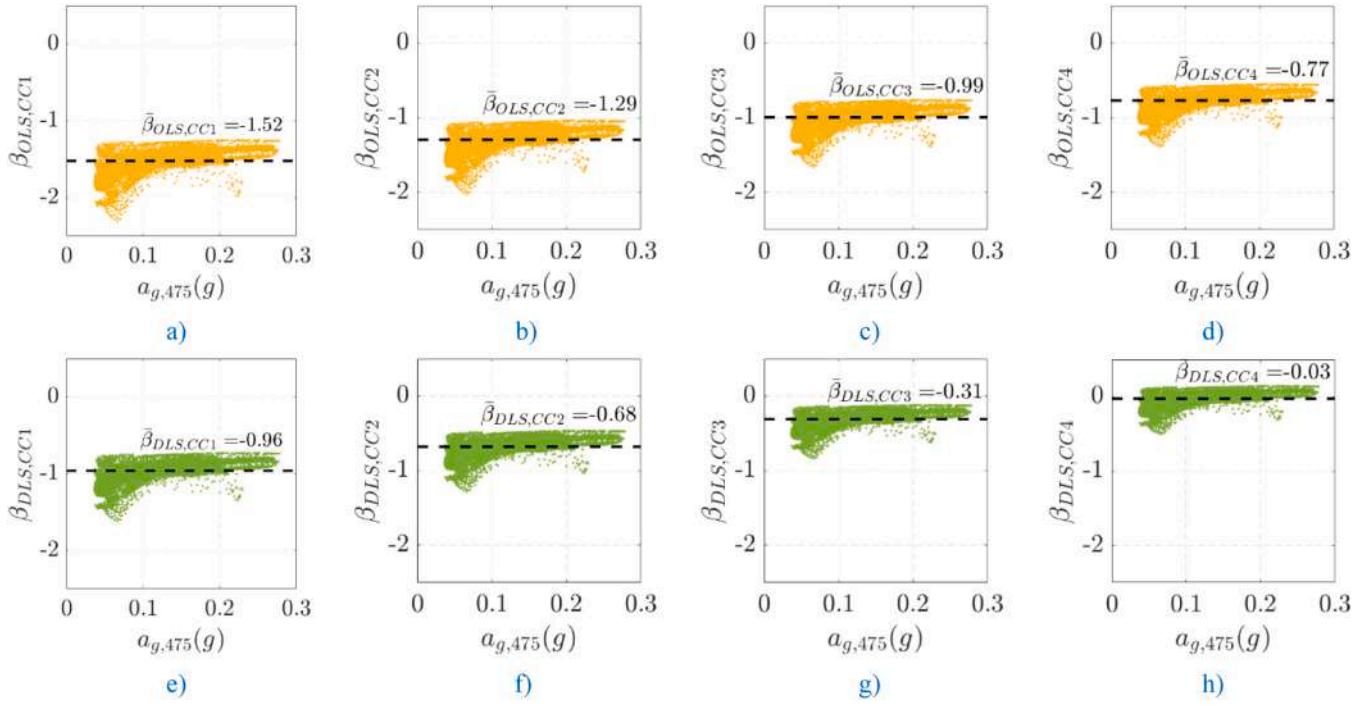

Fig. 17. Target reliability indexes for *SLS* ($\bar{\beta}_{SLS,CC}$) across Italian territory sorted by $a_{g,475}$, assuming $\gamma_{edp} = 1.00$, $\sigma_{\ln,SLS} = 0.32$, and $b = 1$: a-d) *OLS* for *CC1-CC4*; e-h) *DLS* for *CC1-CC4*. Horizontal lines indicate mean values.

is found for all the *ULSs* and *CCs*. For completeness, Fig. 18b plots the mean value $\gamma_{edp}(\bar{\beta}_{LS,CC})$ for both *LSLS* and *CPLS* and from *CC1* to *CC4* (red dots), and the interval mean value $+/-$ one standard deviation (blue dots), evaluated across the entire national territory. It is obvious to note that the $\gamma_{edp}(\bar{\beta}_{LS,CC})$ mean value is constant for both *ULSs* and for the four *CCs*, since it has been assumed constant for calibrating $\bar{\beta}_{LS,CC}$.

Finally, as example Fig. 19 illustrates the Italian map of the $\gamma_{edp}(\bar{\beta}_{LSLS,CC2})$ values (plotted in Fig. 18a). Whereas, Fig. 19b shows the map of $\gamma'_{edp}(\bar{\beta}_{LSLS,CC2})$ reduced by $\gamma_0 = 2.11$ (Table 8). One may clearly note that when $\gamma_0 = 2.11$ is considered, $\gamma_{edp}(\bar{\beta}_{LSLS,CC2})$ may achieve values varying between 1.15 and 0.95. This means that the maximum spectral acceleration may increase up to 15 % particularly for low-

Table 8
$\overline{\beta}_{ULS,CC}$ for *ULS* (*LSLS* and *CPLS*) across four *CCs*, derived as mean values over the Italian territory.

$\overline{\beta}_{ULS,CC}$	Consequence Class (CC) - Consequence of failure			
	***CC1* (Small)**	***CC2* (Some)**	***CC3* (Moderate)**	***CC4* (Great)**
LSLS	1.25	1.63	2.17	2.58
CPLS	1.54	1.96	2.58	2.97

Table 9
$\overline{\beta}_{SLS,CC}$ for *SLS* (*OLS* and *DLS*) across four *CCs*, derived as mean values over the Italian territory.

$\overline{\beta}_{SLS,CC}$	Consequence Class (CC) - Consequence of failure			
	***CC1* (Small)**	***CC2* (Some)**	***CC3* (Moderate)**	***CC4* (Great)**
OLS	-1.52	-1.29	-0.99	-0.77
DLS	-0.96	-0.68	-0.31	-0.03

Table 10
$\overline{\beta}_{DLS,CC}$ for *DLS* considering alternative return periods: $T_R = 95$ years [1] and $T_R = 225$ years [73] for comparison with Eurocode provisions.

$\overline{\beta}_{DLS,CC}$	Consequence Class (CC) - Consequence of failure			
	***CC1* (Small)**	***CC2* (Some)**	***CC3* (Moderate)**	***CC4* (Great)**
$T_R = 95$ years	-0.68	-0.31	0.06	0.30
$T_R = 225$ years	0.37	0.62	0.88	1.04

hazard sites ($a_g < 0.1g$) or may slightly reduce down to 5 % in the case of *LSLS* ($P_E = 10\%$).

As for the *SLSs*, for brevity Fig. 20a reports as example the Italy map of the $\gamma_{edp}(\overline{\beta}_{DLS,CC2})$ values resulting from $\overline{\beta}_{DLS,CC2} = -0.68$ (Table 9). While, in Fig. 20b these values are sorted by the corresponding $a_{g,475}$. It is clear to observe that $\gamma_{edp}(\overline{\beta}_{DLS,CC2})$ may lead to a *DLS* ($P_E = 63\%$) seismic action increment up to 15 %, or to a reduction down to 10 %.

6. Seismic risk analysis: procedure and application to Italian territory

Seismic risk quantifies the potential damage of an asset located in a specific region and for a time period. It is determined starting from three factors, that are: the seismic hazard relating the ground motion intensity *im* to the $\lambda_H(im)$; the asset vulnerability, expressed by its fragility curves; and the exposure, describing the quality and quantity of the asset at risk [74]. The latter may be expressed as a consequence function, providing a *Reconstruction Cost* percentage (%*RC*) for each *LS*. In this study, the consequence function provided into the Ministerial Decree n. 65 [75] is adopted, derived from the reconstruction costs found in Dolce & Manfredi [76]. These values are reported in Table 11.

Usually, the parameter adopted for the seismic risk evaluation is the *Expected Annual Loss* (*EAL*), quantifying the average annual loss considering all the seismic action frequencies. It is provided from the loss curve, depending on the damage probability curves $P(LS = LS_k|IM)$ derived from the fragility ones $P(LS \geq LS_k|IM)$ [77]. $P(LS = LS_k|IM)$ identifies the probability of a certain damage, or *LS*, being reached at specified intensity measure. The damage probability curves are expressed with Eq. 28:

$$P(LS = LS_k|IM) = \begin{cases} 1 - P(LS \geq LS_k|IM) & k = 0 \\ P(LS \geq LS_k|IM) - P(LS \geq LS_{k+1}|IM) & 0 < k \leq n-1 \\ P(LS \geq LS_k|IM) & k = n \end{cases} \quad (28)$$

where LS_k is the *k-th* limit state, in which LS_n correspond to the highest limit state, i.e. *Collapse Limit State* (*CLS*), while LS_0 is the lowest limit state, that is the *Initial Damage Limit State* (*IDLS*).

Once the $P(LS = LS_k|IM)$ is calculated, an economic loss curve $L_{LS}(LS = LS_k|IM)$ may be derived by multiplying the consequence function (Table 11) to each damage probability curve (Eq. 28). It is important to note that these curves are independent on the seismic hazard of a specific site.

Subsequently, the economic loss curve $L_{LS}(LS = LS_k|\lambda_H)$ is the specific site exceedance annual rate $\lambda_H(im)$. Then, the *EAL* (Eq. 29) is evaluated through the summation of the partial EAL_k, calculated as the area below each economic loss curve [78]:

$$EAL = \sum_{LS} EAL_k = \sum_{LS} \int L_{LS}(LS = LS_k|\lambda_H) \bullet d\,\lambda_H \quad (29)$$

where λ_H is the hazard law according in this study to the Bradley et al. [15] formulation.

Fig. 21 reports the result of the seismic risk assessment carried out on the Italian territory. In particular, in each grid point of the national territory and for each *CC*, the *EAL* is calculated (Eq. 29) considering the reliability-targeted capacity fragility curves obtained through $\gamma_{edp}(\overline{\beta}_{LS,CC})$ (Eq. 15), according to $\overline{\beta}_{ULS,CC}$ (Table 8) and $\overline{\beta}_{SLS,CC}$ (Table 9) proposed. Also, Fig. 21 shows the corresponding $\overline{EAL}$ value (red dotted line), derived by imposing that the capacity fragility curves satisfy the target reliability indexes $\overline{\beta}_{LS,CC}$ derived in Sect. 4.5. To do this, the

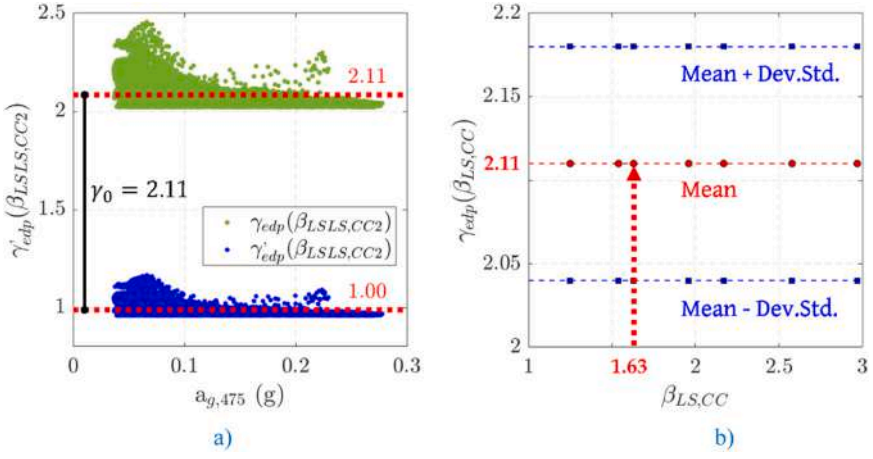

Fig. 18. Target reliability factors for seismic action calibration: a) $\gamma_{edp}(\overline{\beta}_{LSLS,CC2})$ sorted by $a_{g,475}$ for all Italian grid points (green dots) and γ'_{edp} with $\gamma_0 = 2.11$ (blue dots); b) mean values and standard deviation intervals of $\gamma_{edp}(\overline{\beta}_{LS,CC})$ for both *ULS* (*LSLS*, *CPLS*) across four *CCs*.

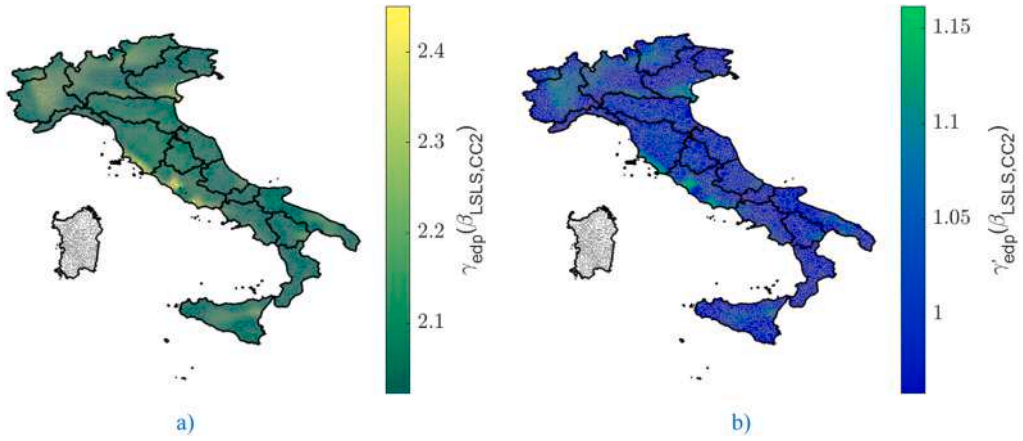

Fig. 19. Maps of target reliability factors for *LSLS* and *CC2* over Italian territory: a) $\gamma_{edp}(\overline{\beta}_{LSLS,CC2})$ ranging from approximately 1.8–2.4; b) overstrength-reduced factor $\gamma'_{edp}(\overline{\beta}_{LSLS,CC2})$ with $\gamma_0 = 2.11$, ranging from 0.95 to 1.15.

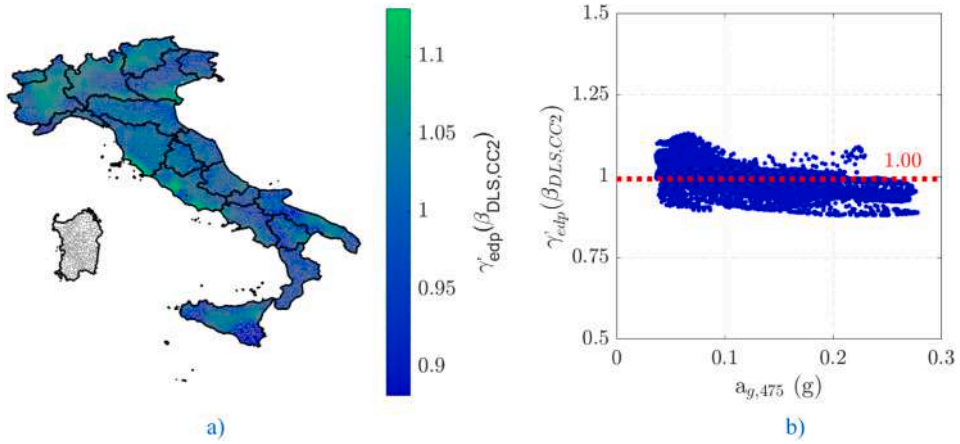

Fig. 20. Target reliability factors for *DLS* and *CC2*: a) map showing $\gamma_{edp}(\overline{\beta}_{DLS,CC2})$ ranging from 0.90 to 1.15 over Italian territory; b) values sorted by acceleration $a_{g,475}$.

Table 11
Consequence function correlating *LS* with economic losses expressed as percentage of Reconstruction Cost (%*RC*).

Limit state description	*Limit State*	%*RC*
Initial Damage	IDLS	0 %
Operativity	OLS	7 %
Damage	DLS	15 %
Life Safety	LSLS	50 %
Collapse prevention	CPLS	80 %
Collapse	CLS	100 %

convolution integral (Eq. 1) is used where the annual reliability index corresponding to P_{f1} is required. It may be derived from the failure probability P_f corresponding to $\overline{\beta}_{ULS,CC}$ (Table 8) and $\overline{\beta}_{SLS,CC}$ (Table 9) proposed (Sect. 4.5) for $t_{ref} > 1$ year (Eq. 11). Note that the *CLS* is not considered in the analysis, since no target reliability index for this *LS* is available. The $\overline{EAL}$ values result constant over the entire national territory since they depend on capacity fragility curves satisfying site-by-site the $\overline{\beta}_{LS,CC}$ values for all the *LSs* considered. Therefore, starting from a reliability-targeted seismic design, i.e. implying target reliability indexes ($\overline{\beta}_{LS,CC}$), a uniform seismic risk is obtained. As one may observe, the *EAL* values (black dots) tend to stabilize more and more around the corresponding $\overline{EAL}$ value from *CC1* to *CC4*. It is also worth noting that in Fig. 21a-d the *EAL* values are consistently lower than the $\overline{EAL}$ ones. This means that the closed-form formulation of $\gamma_{edp}(\overline{\beta}_{LS,CC})$ (Eq. 15) leads to a more conservative approach for the seismic risk estimation.

Moreover, Fig. 22 compares the $\overline{EAL}$ values with the EAL^* ones, where the EAL^* is calculated by considering an amplification factor, constant over the Italian national territory, applied to the design spectrum according to the *MPS-04* maps [60]. In particular, an amplification factor γ_{ULS} equal to 1.0, 1.5 and 2.0 for *ULSs* (*LSLS*, *CPLS*), and γ_{SLS} equal to 1.00 for *SLSs* (*OLS*, *DLS*) is assumed. In the case of the amplification factor equal to 1.00 for both *ULSs* and *SLSs* the *UHA* is adopted. One may note that the higher the amplification factor the lower the scatter with respect to the $\overline{EAL}$ values. This means that, if a *UHA* is followed according to the *MPS-04* maps, that is the current NTC-18 approach [3], the resulting seismic risk expressed in terms of *EALs* results always not uniform over the national territory varying site-by-site and higher than the uniform value obtained according to the target reliability indexes $\overline{\beta}_{ULS,CC}$ and $\overline{\beta}_{SLS,CC}$ proposed.

7. Conclusions

In this paper a reliability-based procedure for calibrating the design seismic action of constructions was presented. The procedure is proposed starting from the approach reported in FEMA [10] and found in Cornell et al. [11] permitting to satisfy, for a given *LS*, a specific reliability requirement expressed through a failure probability. Also, starting from the current *MPS-04* seismic hazard model, the procedure

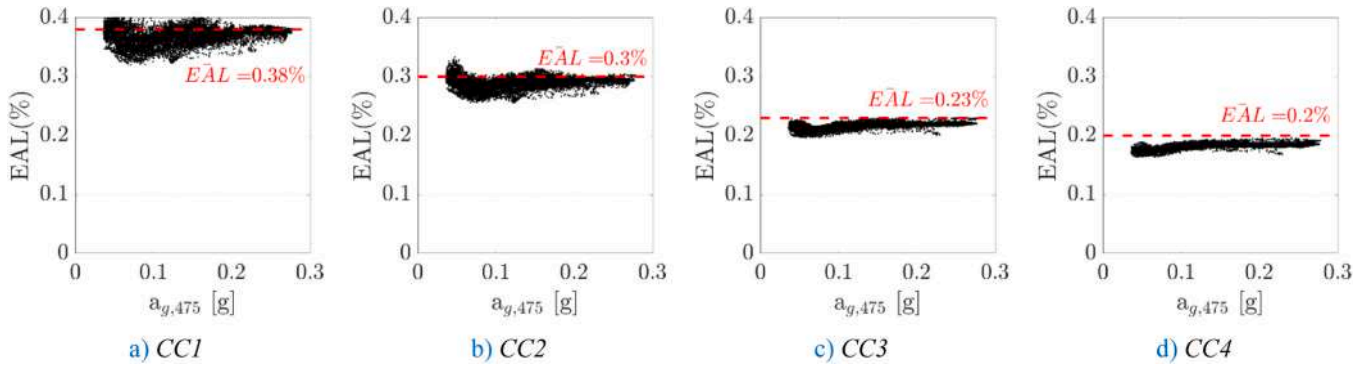

Fig. 21. *EAL* values calculated using reliability-targeted fragility curves with closed-form (black dots) compared with target *EAL* (red dashed line) derived from target reliability indexes $\overline{\beta}_{LS,CC}$ for a) *CC1*, b) *CC2*, c) *CC3*, and d) *CC4* across all Italian grid points sorted by $a_{g,475}$.

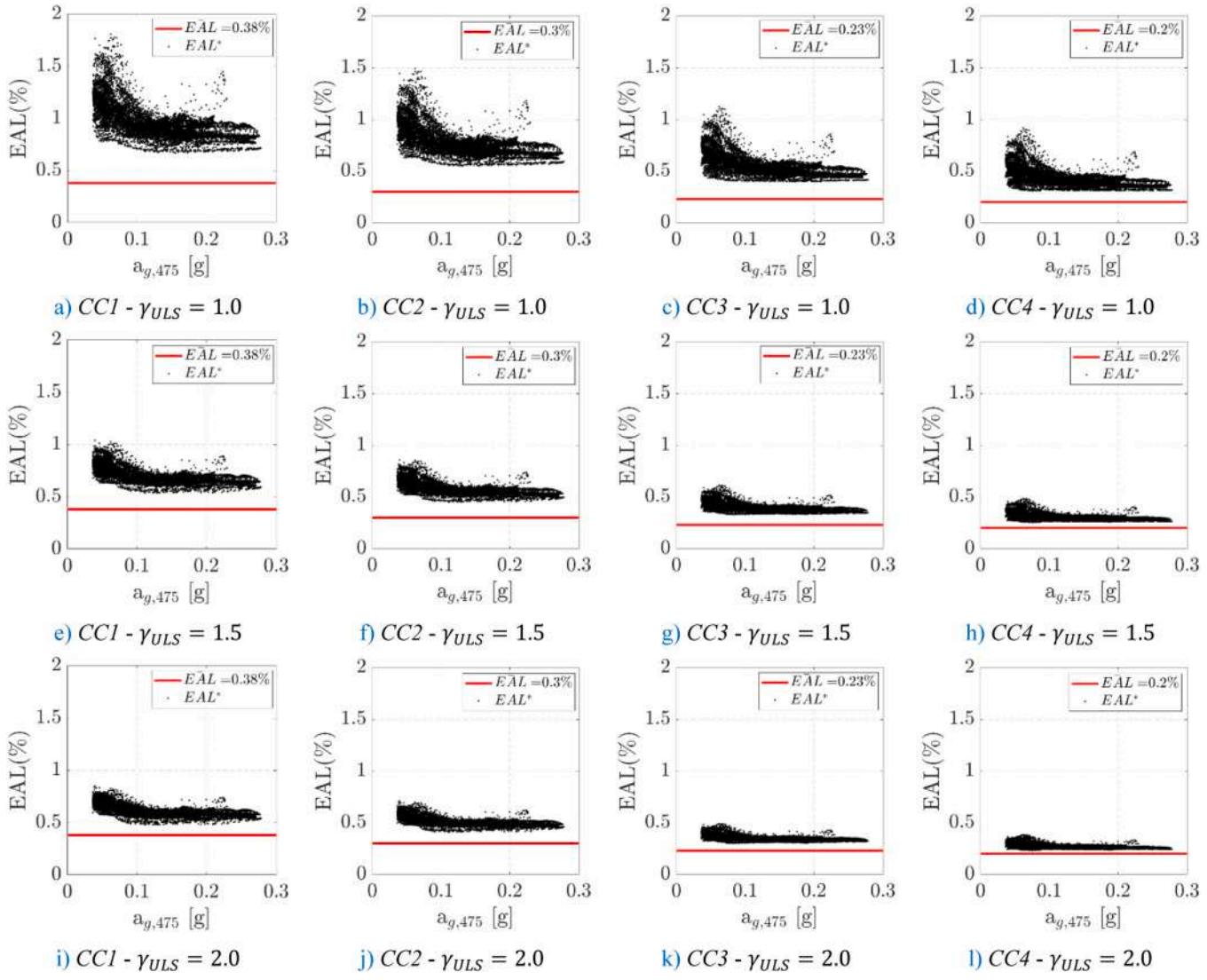

Fig. 22. Comparison of *EAL* under different design approaches: EAL^* calculated with uniform amplification factors (γ_{ULS}= 1.0, 1.5, 2.0; γ_{SLS}= 1.0) applied to *MPS-04* spectra versus target $\overline{EAL}$ from reliability-based approach, for *CC1-CC4*. (a-d) current *UHA* (γ_{ULS} = 1.0) showing non-uniform risk; (e-h) γ_{ULS}= 1.5; (i-l) γ_{ULS}= 2.0.

was applied to the Italian territory permitting to propose a reliability-based seismic action not yet available in the current NTC-18 Italian standards. Consequently, the target reliability indexes $\overline{\beta}_{LS,CC}$ were calibrated and the corresponding target reliability factors $\gamma_{edp}(\overline{\beta}_{LS,CC})$ were derived to obtain seismic action spectra from the ones provided with the *UHA* for satisfying specific reliability requirements. Since $\gamma_{edp}(\overline{\beta}_{LS,CC})$ is a seismic action multiplication factor, the proposed procedure is consistent with a reliability-based design framework that employs partial factors for construction designing against gravitational and seismic loads.

Furthermore, an overstrength factor γ_0 was introduced for taking into account the overstrength reserve in constructions, achievable through the partial factors. By quantifying the appropriate value of γ_0 would permit to correctly meet the reliability requirement for a given *LS* and *CC*.

As far as the application on the Italian territory with the *MPS-04* seismic hazard is concerned, the results obtained showed that sites with low seismic hazard show a target reliability factor more dispersed than the one obtained in sites with high seismic hazard. The proposed procedure yields average target reliability factors of 2.11 for *ULS* (*LSLS* and *CPLS*) and 1.0 for *SLS* (*OLS* and *DLS*) across Italian territory by using the *MPS-04* hazard model. Mean target reliability indexes $\overline{\beta}_{LS,CC}$ vary from 1.25 (*LSLS-CC1*) to 2.97 (*CPLS-CC4*) for *ULS* and −1.52 (*OLS-CC1*) to −0.03 (*DLS-CC4*) for *SLS*.

Also, the seismic risk analysis highlighted that if a reliability-based seismic design is adopted then also a uniform seismic risk is obtained. On the contrary, if a *UHA* is followed according to the *MPS-04* maps, the *EALs* results not uniform over the national territory and higher than the uniform value obtained according to the target reliability indexes proposed.

It should be remarked that the results obtained are dependent on the assumptions made in this study. Firstly, the seismic hazard is linearized in a region of interest in log–log plane. As discussed, outside this region this approximation may lead to an overestimation of seismic reliability. Furthermore, representative fragility curves parameters widely used in the literature are adopted, even though they may not fully capture the variability due to different structural typologies (reinforced concrete, masonry, steel, timber structures) and the epistemic uncertainties involved in real seismic design and assessment. In addition, material strengths were referred to mean values, while design standards are generally based on nominal (or characteristic) values, so that the proposed overstrength factor γ_0 should be properly quantified to ensure that reliability requirements are still satisfied. Finally, the calibration was carried out with reference to the average values $\overline{\beta}_{LS,CC}$ over the entire Italian territory, although the adoption of specific fractiles may be more appropriate in some cases. This choice, however, is strongly driven by economic, social and political considerations that must align with the requirements of the competent Authorities. These aspects may affect the absolute numerical values of $\gamma_{edp}\left(\overline{\beta}_{LS,CC}\right)$, although the general conclusions on the benefits of the proposed procedure remain unchanged.

In future several applications may be made by applying the procedure proposed in this paper. Firstly, when the target annual failure probability $\overline{P}_{f1}$ is assigned for all *LSs* and *CCs* then the target reliability indexes $\overline{\beta}_{LS,CC}$ and the corresponding target reliability factors $\gamma_{edp}\left(\overline{\beta}_{LS,CC}\right)$ may be derived.

Also, it should be noted that the procedure proposed was applied by referring to the mean values of $\overline{\beta}_{LS,CC}$ across the Italian territory. Therefore, the corresponding $\gamma_{edp}\left(\overline{\beta}_{LS,CC}\right)$ maybe also derived starting from a specific fractile of the $\overline{\beta}_{LS,CC}$. Finally, further investigations should be done in order to quantify the resulting overstrength factor γ_0 if partial factors are used in the seismic design of constructions. Future applications should include the calibration of target reliability factors depending on specific structural typologies reflecting, consequently, on the seismic reliability.

The procedure proposed provides a practical probabilistic framework for relevant authorities and engineers to define the seismic action in a reliability-based design. Once the overstrength factor γ_0 and the target annual failure probability $\overline{P}_{f1}$ are fixed, the corresponding $\gamma_{edp}\left(\overline{\beta}_{LS,CC}\right)$ can be directly applied to generate site-dependent reliability-based design spectra. By selecting these two parameters, designers can guarantee the desired level of reliability across different sites with different hazard levels. Therefore, γ_0 and $\overline{P}_{f1}$ become essential for applying a reliability-based seismic design framework.

Notation

The following symbols are used in this paper:

C, D	displacement capacity and demand;
$\widehat{C}$, $\widehat{D}$	median displacement values of the capacity and demand fragility curve;
edp	engineering demand parameter;
im	intensity measure;
$\Phi[\bullet]$	standard normal cumulative distribution;
$im_{\widehat{C}}$, $im_{\widehat{D}}$	median intensity measures corresponding to $\widehat{C}$ and $\widehat{D}$;
$\sigma_{\ln}$	logarithmic values standard deviation of the fragility curve lognormally distributed;
$\sigma_{\ln,SLS}$, $\sigma_{\ln,ULS}$	logarithmic values standard deviation of the *SLS* and *ULS* fragility curves lognormally distributed;
$\sigma_{\ln,R}$, $\sigma_{\ln,U}$	logarithmic values standard deviation of the fragility curve lognormally distributed for randomness and epistemic uncertainties;
$\sigma_{\ln,R,SLS}$, $\sigma_{\ln,U,SLS}$	logarithmic values standard deviation of the *ULS* fragility curve lognormally distributed for randomness and epistemic uncertainties;
$\sigma_{\ln,R,ULS}$, $\sigma_{\ln,U,ULS}$	logarithmic values standard deviation of the *SLS* fragility curve lognormally distributed for randomness and epistemic uncertainties;
μ	construction ductility;
a, b	positive constants obtained from numerical regression of non-linear analyses;
λ_D, λ_H	drift demand and seismic hazard curves;
$\lambda_{H,MPS-04}$	exceedance annual rate provided by *MPS-04* hazard maps;
T_R	return period;
$T_{R,LS,CC}$	return period for a certain *LS* and *CC*;
$T_{R,LS,UC}$	return period for a certain *LS* and *UC*;
$\lambda_{H,475}$, $\lambda_{H,2475}$	annual exceedance probabilities, referring to a T_R of 475 and 2475 years;
k_0, k_1	positive constants representing the intercept and slope of λ_H in a log-log plane;
α, $\lambda_{H,asy}$, im_{asy}	constant, horizontal and vertical asymptotes of the hyperbola seismic hazard curve;
t_{ref}	reference period;
V_R	reference period according to the Italian Standard;
C_U	coefficient of use according to the Italian Standard;
T_1	fundamental period of response spectrum;
PGA	peak ground acceleration;
a_g	peak ground acceleration on rigid soil;
$a_{g,475}$	peak ground acceleration on rigid soil referring to a T_R of 475 years;
$S_e(T_1)$	pseudo-acceleration corresponding to the first vibration period T_1;
$S_e(T_1)_{\widehat{C}}$, $S_e(T_1)_{\widehat{D}}$	pseudo-acceleration of capacity and demand corresponding to the first vibration period T_1;
$S_{e,475}$, $S_{e,2475}$	pseudo-acceleration referring to a T_R of 475 and 2475 years;
RSS	residual squared sum
R^2, $R^2_{\max}$, $R^2_{\min}$	coefficient of determination, and that maximum and minimum
P_E	exceedance probability of the seismic action within t_{ref};
$P_{E,LS}$	exceedance probability of the seismic action within t_{ref} for a certain *LS*;
$P_{E,LS,CC}$	exceedance probability of the seismic action within t_{ref} for a certain *LS* and *CC*;
P_{f1}, P_f	annual failure probability and the one in in a certain t_{ref};
$P_{f1,LS,CC}$	annual failure probability for a certain *LS* and *CC* calculated with the seismic hazard law of Sewell, Toro, & McGuire [12]
$\widehat{P}_{f1,LS,CC}$	annual failure probability for a certain *LS* and *CC* calculated with the seismic hazard law of Bradley et al. [15];
$\overline{P}_{f1,NCLS,CC2}$	annual target failure probability for *NCLS* and *CC2*;
β_1, β	annual reliability index and the one in in a certain t_{ref};
$\overline{\beta}_1$, $\overline{\beta}$	target annual reliability index and the one in in a certain t_{ref};
$\overline{\beta}_{1,NCLS,CC2}$	annual target reliability index for *NCLS* and *CC2*;
$\overline{\beta}_{LS,CC}$	target reliability index for a certain *LS* and *CC*;
$\overline{\beta}_{ULS,CC}$, $\overline{\beta}_{SLS,CC}$	target reliability index for *ULS* and *SLS* for a certain *CC*;
r_i	ratio between $P_{f1,LS,CC}$ calculated with the seismic hazard law of Sewell, Toro, & McGuire [12] and Bradley et al. [15];
$\overline{r}$, $\sigma_{\overline{r}}$	mean and the standard deviation of the ratio values r_i calculated on the entire Italian national territory;
γ_{edp}	safety factor
$\gamma_{edp,ULS}$, $\gamma_{edp,SLS}$	safety factor for *ULS* and *SLS*
$\gamma_{edp}(\overline{\beta}_1)$, $\gamma_{edp}(\overline{\beta})$	target reliability factor corresponding to $\overline{\beta}_1$ and $\overline{\beta}$
γ_0	overstrength factor

(*continued on next page*)

(*continued*)

$\gamma'_{edp}(\overline{\beta})$	target reliability factor corresponding to $\overline{\beta}$ for partial factor method
$\gamma_{edp}(\overline{\beta}_{1,NCLS,CC2})$	target reliability factor corresponding to $\overline{\beta}_{1,NCLS,CC2}$
$f^{rc}(k_0, k_1, \gamma_{edp})$	objective function for k_0 and k_1
$\%RC$	reconstruction cost
L_{LS}	economic loss curve
EAL	expected annual loss
$\overline{EAL}$	EAL derived with the by imposing that the fragility curves satisfy the target reliability indexes $\overline{\beta}_{LS,CC}$
γ_{ULS}, γ_{SLS}	amplification factor of response spectrum for ULS and SLS
EAL^*	EAL calculated by considering a constant value of amplification factor γ_{ULS} and γ_{SLS}

Author contribution

All Authors contributed equally to this manuscript.

CRediT authorship contribution statement

All Authors contributed equally to this manuscript.

Declaration of Competing Interest

The Authors declare that they received no funds, grants or other support during the preparation of this manuscript.

Data availability

Data will be made available on request.

References

[1] EN 1998-1, 2004. Eurocode 8: design of structures for earthquake resistance—Part 1: general rules, seismic actions and rules for buildings, EN 1998–1. European Committee for Standardisation: Brussels, 2004.

[2] ICBO, 1997. Uniform Building Code. USA: International Council of Building Officials.

[3] NTC-18, 2018. D.M. 17.01.18. Aggiornamento delle 'Norme Tecniche per le costruzioni.' Rome: Italian Ministry of Infrastructure. (In Italian).

[4] Costa A, Romão X, Oliveira CS. A methodology for the probabilistic assessment of behaviour factors. Bull Earthq Eng 2010;8(1):47–64. https://doi.org/10.1007/s10518-009-9126-5.

[5] Iervolino I, Spillatura A, Bazzurro P. Seismic reliability of code-conforming Italian buildings. J Earthq Eng 2018;22:5–27. https://doi.org/10.1080/13632469.2018.1540372.

[6] Baltzopoulos G, Grella A, Iervolino I. Some issues in the practical application of risk-targeted ground motions. Earthq Eng Struct Dyn 2023;53:997–1005. https://doi.org/10.1002/eqe.4058.

[7] Žižmond J, Dolšek M. Formulation of risk-targeted seismic action for the force-based seismic design of structures. Earthq Eng Struct Dyn 2019;48:1406–28. https://doi.org/10.1002/eqe.3206.

[8] Cornell CA, Krawinkler H. Progress and challenges in seismic performance assessment. PEER Cent N 2000. ⟨https://apps.peer.berkeley.edu/news/2000spring/performance.html⟩.

[9] Kennedy RP. Risk based seismic design criteria. Nucl Eng Des 1999;192. https://doi.org/10.1016/S0029-5493(99)00102-8. ⟨www.elsevier.com/locate/nucengdes⟩.

[10] FEMA, 2000. Recommended seismic design criteria for new steel moment frame buildings. Report No. FEMA 350, SAC Joint Venture, Federal Emergency Management Agency, Washington, DC.

[11] Cornell CA, Jalayer F, Hamburger RO, Foutch DA. Probabilistic basis for 2000 SAC federal emergency management agency steel moment frame guidelines. J Struct Eng 2002. https://doi.org/10.1061/(ASCE)0733-9445(2002)128:4(526).

[12] Sewell, R.T., Toro, G.R., & McGuire, R.K., 1991. Impact of ground motion characterisation on conservatism and variability in seismic risk estimates. NUREG/CR-6467, U.S. Nuclear Regulatory Commission, Washington, DC.

[13] Aslani H, Miranda E. Probability-based seismic response analysis. Eng Struct 2005;27(8):1151–63.

[14] Bradley BA, Dhakal RP. Error estimation of closed-form solution for annual rate of structural collapse. Earthq Eng Struct Dyn 2008;37(15):1721.

[15] Bradley BA, Dhakal RP, Cubrinovski M, Mander JB, MacRae GA. Improved seismic hazard model with application to probabilistic seismic demand analysis. Earthq Eng Struct Dyn 2007;36:2211–25. https://doi.org/10.1002/eqe.727.

[16] Vamvatsikos D. Derivation of new SAC/FEMA performance evaluation solutions with second-order hazard approximation. Earthq Eng Struct Dyn 2013;42(8):1171–88. https://doi.org/10.1002/eqe.2265.

[17] Torres MA, Ruiz SE. Structural reliability evaluation considering capacity degradation over time. Eng Struct 2007;29:2183–92. https://doi.org/10.1016/j.engstruct. 2006. 11. 014.

[18] Celarec D, Vamvatsikos D, Dolšek M. Simplified estimation of seismic risk for reinforced concrete buildings with consideration of corrosion over time. Bull Earthq Eng 2011;9:1137–55. https://doi.org/10.1007/s10518-010-9241-3.

[19] Vamvatsikos D, Dolšek M. Equivalent constant rates for performance-based seismic assessment of ageing structures. Struct Saf 2011;33:8–18. https://doi.org/10.1016/j.strusafe.2010.04.005.

[20] Tolentino D, Ruiz S,E, Torres MA. Simplified closed-form expressions for the mean failure rate of structures considering structural deterioration. Struct Infrastruct Eng 2012;8:483–96. https://doi.org/10.1080/15732479.2010.539067.

[21] Tolentino D, Ruiz SE. Time-dependent confidence factor for structures with cumulative damage. Earthq Spectra 2015;31:441–61. https://doi.org/10.1193/010912EQS0 08M.

[22] Celarec D, Dolšek M. Practice-oriented probabilistic seismic performance assessment of infilled frames with consideration of shear failure of columns. Earthq Eng Struct Dyn 2013;42:1339–60. https://doi.org/10.1002/eqe.2275.

[23] Fragiadakis M, Vamvatsikos D, Karlaftis MG, et al. Seismic assessment of structures and lifelines. J Sound Vib 2015;334:29–56. https://doi.org/10.1016/j.jsv.2013.12.031.

[24] Flores RB, Tolentino D. Simplified estimation of reliability in structures subjected to seismic loads using the demand-capacity ratio format. Bull Earthq Eng 2024;22:4635–55. https://doi.org/10.1007/s10518-024-01923-y.

[25] Ellingwood BR. Earthquake risk assessment of building structures. Reliab Eng Syst Saf 2001;74:251–62. https://doi.org/10.1016/S0951-8320(01)00105-3.

[26] Tatangelo M, Audisio L, D'Amato M, Gigliotti R. Issues related to typological fragility curves derivation starting from observed seismic damage. Eng Struct 2024;307:17853. https://doi.org/10.1016/j.engstruct.2024.117853.

[27] Vamvatsikos D, Cornell AC. Incremental dynamic analysis. Earthq Eng Struct Dyn 2002;31(3):491–514. https://doi.org/10.1002/eqe.141.

[28] Jalayer F, Cornell CA. Alternative non-linear demand estimation methods for probability-based seismic assessments. Earthq Eng Struct Dyn 2009;38(8):951–72.

[29] Jalayer F, Ebrahimian H, Miano A, Manfredi G, Sezen H. Analytical fragility assessment using unscaled ground motion records. Earthq Eng Struct Dyn 2017;46(15):2639–63. https://doi.org/10.1002/eqe.2922.

[30] Baltzopoulos G, Baraschino R, Iervolino I, Vamvatsikos D. SPO2FRAG: software for seismic fragility assessment based on static pushover. Bull Earthq Eng 2017;15(10):4399–425. https://doi.org/10.1007/s10518-017-0145-3.

[31] Vamvatsikos D, Cornell CA. Direct estimation of the seismic demand and capacity of oscillators with multi-linear static pushovers through IDA. Earthq Eng Struct Dyn 2006;35(9):1097–117. https://doi.org/10.1002/eqe.573.

[32] Dolšek M, Fajfar P. IN2 – A Simple Alternative for IDA. Proceedings of the 13th World Conference on Earthquake Engineering, Vancouver, Canada. 2004. p. 3353.

[33] Dolšek M, Fajfar P. Simplified probabilistic seismic performance assessment of plan-asymmetric buildings. Earthq Eng Struct Dyn 2007;36(13):2021–41.

[34] Fajfar P, Dolšek M. A practice-oriented estimation of the failure probability of building structures. Earthq Engng Struct Dyn 2012;41:531–47.

[35] Bilgin H, Shkodrani N, Hysenlliu M, Ozmen HB, Isik E, Harirchian E. Damage and performance evaluation of masonry buildings constructed in 1970s during the 2019 Albania earthquakes. Eng Fail Anal 2022;131:105824. https://doi.org/10.1016/j.engfailanal.2021.105824.

[36] Ademovic N, Toholj M, Radonic D, Casarin F, Komesar S, Ugarkovic K. Post-earthquake assessment and strengthening of a cultural-heritage residential masonry building after the 2020 zagreb earthquake. Buildings 2022 2022;12(11):2024. https://doi.org/10.3390/buildings12112024.

[37] Bai W, Shao Z, Dai J, Yang Y. Earthquake damage reconnaissance and numerical analysis of a middle school teaching building after the Ms 6.0 Changning earthquake. Eng Fail Anal 2025;169:109201. https://doi.org/10.1016/j.engfailanal.2024.109201.

[38] Fuentes DD, Baquedano Julià PA, D'Amato M, Laterza M. Preliminary seismic damage assessment of Mexican churches after September 2017 earthquakes. Int J Archit Herit 2021;15(4):505–25.

[39] Palazzi NC, Favier P, Rovero L, Sandoval C, de la Llera JC. Seismic damage and fragility assessment of ancient masonry churches located in central Chile. Bull Earthq Eng 2020;18:3433–57. https://doi.org/10.1007/s10518-020-00831-1.

[40] D'Amato M, Laguardia R, Di Trocchio G, Coltellacci M, Gigliotti R. Seismic risk assessment for masonry buildings typologies from L'Aquila 2009 earthquake damage data. J Earthq Eng 2022;26(9):4545–79. https://doi.org/10.1080/13632469.2020.1835750.

[41] Laguardia R, D'Amato M, Coltellacci M, Di Trocchio G, Gigliotti R. Fragility curves and economic loss assessment of RC buildings after L'Aquila 2009 earthquake. J Earthq Eng 2023;27(5):1126–50. https://doi.org/10.1080/13632469.2022.2038726.

[42] Tatangelo, M., Audisio, L., D'Amato, M., & Gigliotti, R., 2023b. Typological seismic losses assess-ment by damaged masonry buildings after L'Aquila 2009 and Emilia 2012 earthquakes. In: Proceedings of the 9th ECCOMAS Thematic Conference on Computational Meth-ods in Structural Dynamics and Earthquake Engineering, pp. 1071–1083, Athens, Greece, 2023. DOI: (⟨https://doi.org/10.7712/120123.10458.20639⟩.

[43] Castaldo P, Ferrentino Tatiana. Seismic reliability-based design approach for base-isolated systems in different sites. Sustainability 2020 2020;12:2400. https://doi.org/10.3390/su12062400.

[44] Micozzi F, Scozzese F, Ragni L, Dall'Asta A. Seismic reliability of base isolated systems: sensitivity to design choices. Eng Struct 2022;256:114056. https://doi.org/10.1016/j.engstruct.2022.114056.

[45] De Iuliis M, Miceli E, Castaldo P. Information theory-guided machine learning to estimate seismic response of non-linear SDOF structures. Eng Struct 2025;336:120448.
[46] Dolšek M, Lazar Sinković N, Žižmond J. IM-based and EDP-based decision models for the verification of the seismic collapse safety of buildings. Earthq Eng Struct Dyn 2017;46(15):1–18. https://doi.org/10.1002/eqe.2923.
[47] ASCE, 2016. Asce/sei 7-16 Minimum Design Loads and Associated Criteria for Buildings and Other Structures. (American Society of Civil Engineers, 2016).
[48] Model Code, 2020. fib Model Code for concrete structures (2020). Fédération Internationale du Béton.
[49] CEN, 2022. Technical Committee 250 Sub-Committee 8. prEN 1998-1-1.
[50] Douglas J, Ulrich T, Negulescu C. Risk-targeted seismic design maps for mainland France. Nat Hazards 2013;65(3):1999–2013. https://doi.org/10.1007/s11069-012-0460-6.
[51] Kharazian A, Molina S, Galiana-Merino JJ, Agea-Medina N. Risk-targeted hazard maps for Spain. Bull Earthq Eng 2021;19:5369–89. https://doi.org/10.1007/s10518-021-01189-8.
[52] Monti G, Demartino C, Gardoni P. Towards risk-targeted seismic hazard models for Europe. Sci Rep 2023;13:10717. https://doi.org/10.1038/s41598-023-36947-y.
[53] Zhang M, Pan H, Zhang Y. Towards national risk-targeted seismic hazard maps for mainland China. Geomat Nat Hazards Risk 2025;16(1):2475880. https://doi.org/10.1080/19475705.2025.2475880.
[54] Horspool N, Hulsey A, Elwood K, Gerstenberger M. Risk-targeted hazard for seismic design in New Zealand considering individual and societal risk targets. Earthq Spectra 2023;39(2):1007–36. https://doi.org/10.1177/87552930231156947.18.
[55] Hulsey AM, Horspool N, Gerstenberger MC, Sullivan TJ, Elwood KJ. Considering uncer-tainty in the collapse fragility of New Zealand buildings for risk-targeted seismic design. Earthq Engng Struct Dyn 2023;52(13):4205–21. https://doi.org/10.1002/eqe.3916.
[56] Zarrineghbal A, Zafarani H, Rahimian M. Towards an Iranian national risk-targeted model for seismic hazard mapping. Soil Dyn Earthq Eng 2021;141:106495. https://doi.org/10.1016/j.soildyn.2020.106495.
[57] Zarrineghbal A, Zafarani H, Rahimian M, Jalalalhosseini SM, Khanmohammadi M. Risk-targeted seismic design maps with aleatory and epistemic uncertainty in Tehran and sur-rounding areas. J Earthq Eng 2024;28(14):3925–53. https://doi.org/10.1080/13632469.2024.2368179.20.
[58] Luco N, Ellingwood BR, Hamburger RO, Hooper JD, Kimball JK, Kircher C. Risk-targeted versus current seismic design maps for the conterminous united states. Struct Eng Assoc Calif 2007 Conv Proc 2007.
[59] Franchin P, Noto F. Reliability-based partial factors for seismic design and assessment consistent with second-generation Eurocode 8. Earthq Engng Struct Dyn 2023;52:4026–47. https://doi.org/10.1002/eqe.3840.
[60] Stucchi M, Meletti C, Montaldo V, Akinci A, Faccioli E, Gasperini P, et al. Pericolosità sismica di riferimento per il territorio nazionale MPS04. Ist Naz di Geofis e Vulcanol (INGV) 2004. https://doi.org/10.13127/sh/mps04/ag.
[61] Benjamin JR, Cornell CA. Probability, statistics, and decision for civil engineers. New York: McGraw-Hill; 1970.
[62] Franchin P, Petrini F, Mollaioli F. Improved risk-targeted performance-based seismic design of reinforced concrete frame structures. Earthq Eng Struct Dyn 2018;47:49–67. https://doi.org/10.1002/eqe.2936.
[63] Tatangelo M, Audisio L, D'Amato M, Gigliotti R, Braga F. A new reliability-based procedure for life-cycle management of new and existing constructions. Structures 2024;70:107837. https://doi.org/10.1016/j.istruc.2024.107837.
[64] Cornell CA. A probability based structural code. J Am Concr Inst 1969;66(12):974–85.
[65] FEMA P-695, 2009. Quantification of Building Seismic Performance Factors. Report No. FEMA P695, Federal Emergency Management Agency, Washington, DC.
[66] Dolšek M, Fajfar P. Inelastic spectra for infilled reinforced concrete frames. Earthq Eng Struct Dyn 2004;33(15):1395–416.
[67] Vamvatsikos D, Fragiadakis M. Incremental dynamic analysis for estimating seismic performance sensitivity and uncertainty. Earthq Eng Struct Dyn 2010;39(8):141–63.
[68] Zareian F, Krawinkler H, Ibarra L, Lignos D. Basic concepts and performance measures in prediction of collapse of buildings under earthquake ground motions. Struct Des Tall Spec Build 2010;19:167–81.
[69] Liel AB, Haselton CB, Deierlein GG, Baker JW. Incorporating modeling uncertainties in the assessment of seismic collapse risk of buildings. Struct Saf 2009;31(2):197–211.
[70] Castaldo P, Gino D, Bertagnoli G, Mancini G. Resistance model uncertainty in non-linear finite element analyses of cyclically loaded reinforced concrete systems. Eng Struct 2020;211:110496. https://doi.org/10.1016/j.engstruct.2020.110496.
[71] Willett JB, Singer JD. Another cautionary note about R2: its use in weighted least-squares regression analysis. Am Stat 1988;42(3):236–8.
[72] OPCM 3274, 2003. Ordinanza 20/03/03. Primi elementi in materia di criteri generali per la classificazione sismica del territorio nazionale e di normative tecniche per le costruzioni in zona sismica. Rome: Italian Ministry of Infrastructure. (In Italian).
[73] EN 1998-3, 2005. Eurocode 8: Design of structures for earthquake resistance – Part 3: Assessment and retrofitting of buildings. EN 1998–3. European Committee for Standardisation: Brussels, 2005.
[74] Dolce M, Prota A, Borzi B, da Porto F, Lagomarsino S, Magenes G, et al. Seismic risk assessment of residential buildings in Italy. Bull Earthq Eng 2021;19:2999–3032. https://doi.org/10.1007/s10518-020-01009-5.
[75] Ministerial Decree n. 65, D.M. 7 July 2017. Linee Guida per la Classificazione del Rischio Sismico delle Costruzioni (In Italian).
[76] Dolce, M., & Manfredi, G., 2015. Libro bianco sulla ricostruzione privata fuori dai centri storici nei comuni colpiti dal sisma dell'Abruzzo del 6 Aprile 2009. Rome (IT). (In Italian).
[77] Tatangelo M, Audisio L, D'Amato M, Gigliotti R. Seismic risk analysis on masonry buildings damaged by L'Aquila 2009 and Emilia 2012 earthquakes. Procedia Struct Integr 2023;44:990–7. https://doi.org/10.1016/j.prostr.2023.01.128.
[78] Porter K, Beck JK, Shaikhutdinov R. Simplified estimation of economic seismic risk for buildings. Earthq Spectra 2004;20(4):1239–63. https://doi.org/10.1193/1.1809129.